

# Photo-cross-linked Polypeptide Nanoparticles via ROPISA Methodology

A thesis submitted towards the partial fulfilment of the  
Integrated BS-MS dual degree



Submitted by  
**Akshaya Maria Prasad**  
(Registration No: **20181115**)

Under the guidance of  
**Prof. Manickam Jayakannan**  
Department of Chemistry  
Indian Institute of Science Education and Research, Pune

### Certificate

This is to certify that this dissertation entitled "**Photo-cross-linked Polypeptide Nanoparticles via ROPISA Methodology**" towards the partial fulfilment of the BS-MS dual degree programme at the Indian Institute of Science Education and Research, Pune, represents work carried out by **Akshaya Maria Prasad** at IISER Pune under the supervision of **Prof. Manickam Jayakannan**, Department of Chemistry during the academic year 2022-2023.

Date: 10<sup>th</sup> April, 2023

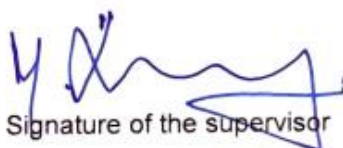
Place: Pune



Signature of the student

Date: 10<sup>th</sup> April, 2023

Place: Pune



Signature of the supervisor

10/4/2023

### Declaration

I hereby declare that the matter embodied in the report entitled "**Photo-cross-linked Polypeptide Nanoparticles via ROPISA Methodology**" are the results of the work carried out by me at the Department of chemistry, IISER Pune, under the supervision of **Prof. Manickam Jayakannan** and the same has not been submitted elsewhere for any other degree.

Date: 10<sup>th</sup> April, 2023

Place: Pune



Signature of the student

Date: 10<sup>th</sup> April, 2023

Place: Pune



Signature of the supervisor

10/4/2023

## **Acknowledgments**

I want to extend my sincere gratitude to my thesis Supervisor Prof. M. Jayakannan, for his constant support, encouragement and guidance. His enthusiasm for research and optimistic outlook always motivated and shaped me to a better person.

I am thankful to my Thesis Advisory Committee (TAC) member Prof. S. G. Srivatsan, for his advice and helpful suggestions during the mid-semester presentation, which helped me make necessary improvements.

Many thanks to Rahul and Parshuram who mentored me during the various stages of my project and Shahid, Ruma, Utreshwar, Kajal, Mansi, Sanchi, Rhujal, Ashutosh, Mishika and Khuddus for their help and support in and out of the lab. My deepest gratitude to Rahul for guiding me, helping me out through each and every problem I faced during my work. I also like to thank Parshuram for his assistance with my work and Shahid for his help with data analysis.

I am incredibly lucky to have a fantastic bunch of friends who have stood with me throughout all my ups and down over the past five years and who made my life at IISER joyful and special.

Lastly but most importantly, my constant support system, my papa, mummy, “chechi” and Tom for their immense love, care and support.

## **Table of contents**

List of Figures and Tables .....	7
Abbreviations .....	8
Abstract .....	9
1. Introduction	
1.1. Polypeptides .....	12
1.2. Ring opening polymerization induced self-assembly (ROPISA) of polypeptides .....	15
1.3. Photo Crosslinking .....	16
1.4. Cinnamoyl group for photo crosslinking .....	18
1.5. Aim of the thesis .....	19
2. Experimental Section	
2.1. Material .....	21
2.2. Methods.....	21
2.3. Synthesis	
2.3.1. Cinnamoyl Serine .....	21
2.3.2. Cinnamoyl L-Serine NCA .....	22
2.3.3. Benzyl L-Glutamate NCA .....	22
2.3.4. CBz-lysine NCA .....	23
2.3.5. Polymer Synthesis	
2.3.5.1. Di-block copolymers: PEG-b-P(CSer) <sub>n</sub> .....	23
2.3.5.2. Tri-block copolymer synthesis .....	24
2.3.6. ROPISA mediated polymerization .....	25
2.3.7. In-situ encapsulation of Dyes via ROPISA .....	26
2.4. CMC measurements .....	27
2.5. Photo crosslinking strategy .....	27
3. Results and Discussion	
3.1. Monomer Synthesis and characterization.....	28
3.2. Optimization of Polymerization in organic solvent .....	31
3.3. Optimization of Polymerization: ROPISA route .....	36
3.4. Size and Morphology .....	40
3.5. Micelle formation and CMC study .....	41

3.6. Photo crosslinking strategy, verification and its effect on size .....	42
3.7. ROPISA driven encapsulation strategy .....	46
4. Conclusion .....	49
5. References .....	50

## **List of Figures and Tables**

Figure 1.1: Self-assembly of block copolymers.....	11
Figure 1.2: PISA – biodegradable and non-biodegradable monomers.....	12
Figure 1.3: Photo crosslinking functional groups.....	17
Figure 1.4: Aim of the thesis.....	20
Figure 3.1: $^1\text{H}$ and $^{13}\text{C}$ NMR of Cinnamoyl serine .....	29
Figure 3.2: FTIR spectrum of monomer, NCA .....	30
Figure 3.3: $^1\text{H}$ NMR of NCA's .....	31
Figure 3.4: FTIR spectra of di-block and tri-block copolymer .....	33
Figure 3.5: $^1\text{H}$ NMR of di-blocks .....	34
Figure 3.6: GPC plots of di-block and triblock copolymer.....	35
Figure 3.7: $^1\text{H}$ NMR of tri-block copolymers .....	36
Figure 3.8: Synthetic scheme and photographs of ROPISA strategy .....	37
Figure 3.9: FTIR spectra of di-blocks via ROPISA .....	38
Figure 3.10: $^1\text{H}$ NMR of di-block copolymers via ROPISA .....	34
Figure 3.11: GPC of di-block copolymers via ROPISA .....	40
Figure 3.12: Size and morphology of ROPISA nano assemblies .....	40
Figure 3.13: Self-assembly verification .....	42
Figure 3.14: Photo crosslinking strategy .....	42
Figure 3.15: UV-Vis spectra of photo crosslinking .....	44
Figure 3.16: DLS histograms of photo crosslinked nanoparticles .....	45
Figure 3.17: TEM and AFM images of crosslinked nano assemblies .....	46
Figure 3.18: ROPISA driven encapsulation strategy .....	46
Figure 3.19: Data for Rhodamine B loaded polymer emulsion .....	47
Figure 3.20: Data for Nile Red loaded polymer emulsion .....	48
Table 3.1: $^1\text{H}$ NMR and GPC characterization table (solvent route) .....	34
Table 3.2: $^1\text{H}$ NMR and GPC characterization table (ROPISA route) .....	40

## **Abbreviations**

- ❖ THF: Tetrahydrofuran
- ❖ DMSO: Dimethyl Sulphoxide
- ❖ NHC: N-Heterocyclic Carbene
- ❖ NCA: N-carboxyanhydride
- ❖ ROP: Ring Opening Polymerization
- ❖ ROPISA: Ring Opening Polymerization Induced Self Assembly
- ❖ CMC: Critical micelle concentration
- ❖ GPC: Gel Permeation Chromatography
- ❖ DLS: Dynamic light Scattering
- ❖ AFM: Atomic force microscopy
- ❖ HR-TEM: High resolution - Transmission electron microscopy
- ❖ MeO-PEG<sub>5000</sub>-NH<sub>2</sub>: Poly (ethylene glycol) methyl ether amine
- ❖ Bn-Glu:  $\gamma$ -Benzyl L-Glutamate
- ❖ CBz-Lys:  $\epsilon$ -CBz L-Lysine
- ❖ PEG-b-P(CSer): Poly (ethylene glycol) methyl ether amine-block-poly (Cinnamoyl Serine)



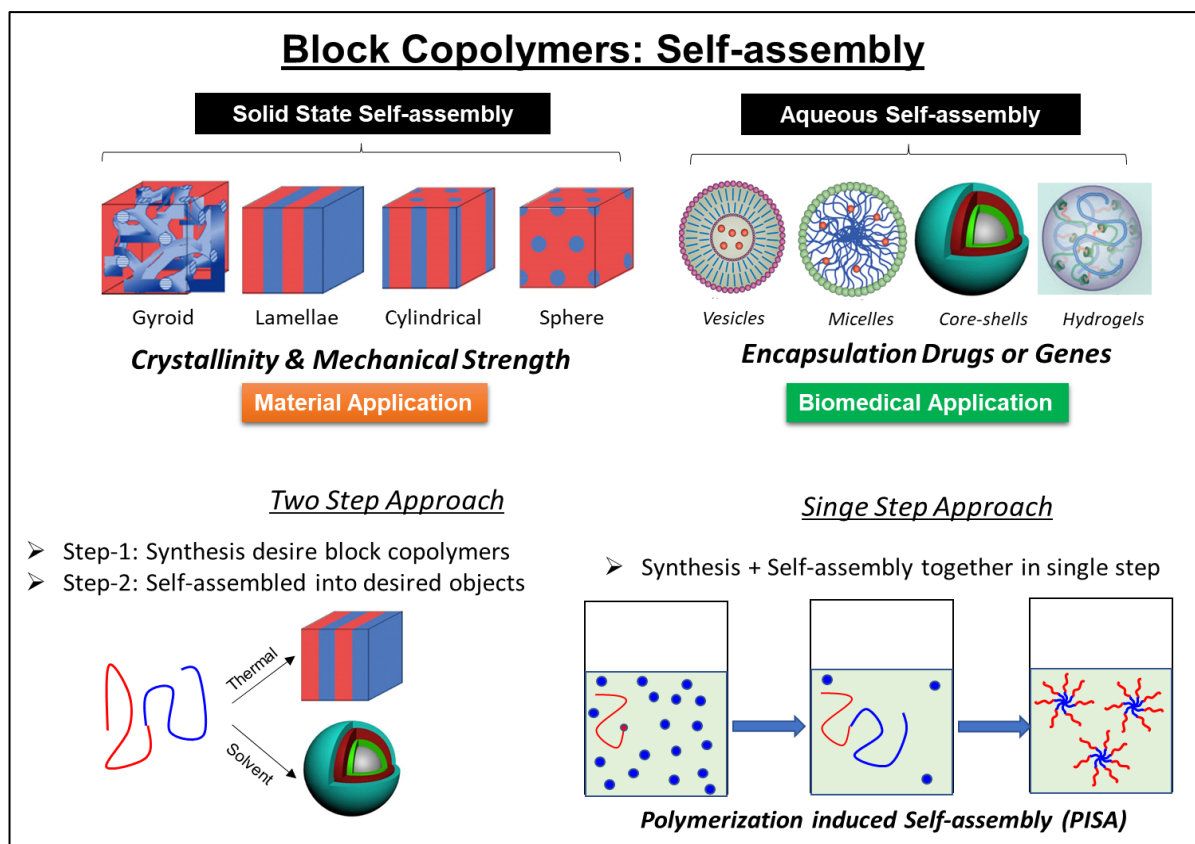
## **Abstract**

Photo-crosslinked polymer nano-assemblies have gained significant importance in biomedical field in drug delivery, and tissue engineering, etc. This thesis work is aimed to make new classes of photo-crosslinkable polypeptides in aqueous medium via polymerization-induced self-assembly process. For this purpose, cinnamoyl functional group was conjugated into L-serine, an amino acid bio-resource, and new N-carboxylic anhydride (NCA) monomer was synthesized. The solvent route polymerization using PEG- amine as an initiator and NHC as catalyst via ring opening polymerization (ROP) confirmed the potential of the serine monomer to form polymers in controlled and efficient manner. The ring opening polymerization induced self-assembly (ROPISA) was employed taking PEG-amine as the hydrophilic initiator, to make stable emulsion of PEG-polypeptide di-block copolymer nano assemblies. ROPISA of serine-NCA monomer at  $M/I = 10$  or  $25$  provided stable polymer emulsions in the form of opalescent solutions. The monomodal, narrow dispersed GPC profile and close agreement between the molecular weight of the amphiphilic di-block copolymers and the anticipated molecular weight of the copolymers indicate controlled polymerization. The size of the nano assemblies in these polypeptide emulsions range between 25 and 30 nm and had a spherical nanoparticle morphology. The photocuring ability of this opalescent solution was examined using UV light of wavelength 265nm. Upon shining the light, the cinnamoyl group underwent [2+2] cyclo addition which was confirmed by UV spectroscopy. The DLS studies revealed that the properties of the nanoparticle produced via ROPISA is intact after curing. Crosslinked and non-crosslinked nanoparticle loading efficiency were studied using dyes like Nile Red and Rhodamine B.

## 1. Introduction

The block-copolymers are the excellent polymeric architectures in which two or more polymeric structures with different chemical structure are covalently connected to each other.<sup>1</sup> Most commonly, block copolymers are synthesized by living polymerization of different monomers in sequential manner on the other hand, copolymerization of various monomers in one pot leads to formation of random copolymers. The presence of different distinct segments having various chemical structures gives unique properties to block copolymers compared to random copolymers. The difference in chemical composition of constituent block segments leads to self-assembly of block copolymer wherein it spontaneously organizes into higher order structures through non-covalent interactions, such as van der waals forces, hydrogen bonding, and electrostatic interactions with defined size and morphology.<sup>2</sup> The self-assembly of block copolymer can take many different forms from simple micelles and vesicles to more complex structures such as nanorods and nanotubes. The self-assembly of block copolymer can occur in either solid state or solution state (Figure 1.1).<sup>3</sup> Solid phase self-assembly is a process when block copolymer molecules spontaneously arrange themselves on a solid surface into the desired form (crystals, thin films, layers, etc.) without the need for external intervention.<sup>4</sup> A wide variety of useful materials, such as sensors, catalysts, and electronic devices, can be produced using this method.<sup>5</sup> In solution state self-assembly block copolymer molecules spontaneously arrange themselves into the higher order structures upon dissolution in suitable solvent. In case of most practical applications, block copolymer acts as amphiphile and self assembles in water as solvent. This aqueous self-assembly of block copolymer can be carried out in two ways. In first method,<sup>6</sup> the amphiphilic block copolymer is synthesized and then self-assembled by means of various ways such as dialysis method, nano-precipitation, film hydration method, etc. This two step-approach is most commonly practiced way of self-assembling block copolymers in to various nano objects like vesicles, micelles, rods, worms, torroids, etc. Although, the two-step approach of block copolymer self-assembly is more common, it is inaccessible to most commercial applications since it is performed under

dilute conditions (concentration is less than 1 wt %) as a result their industrial scalability is not feasible and expensive.



**Figure: 1.1 – Self-assembly of block copolymers**

The another way of self-assembling block copolymers is one step process known as polymerization induced self-assembly (PISA).<sup>7</sup> Commonly, aqueous PISA involves the polymerization of hydrophobic monomer in water using water soluble hydrophilic macroinitiator and it leads to the formation of amphiphilic block copolymer which grows and self-assembles simultaneously in to various kinds of nano objects.<sup>8</sup> The PISA process can also be performed in organic solvents and in that scenario, chain extension of macroinitiator which is soluble in polymerization solvent is done using monomer who's respective homopolymer is not soluble in polymerization solvent.<sup>9</sup> The PISA is known since quite a long time after its report based on it appeared in 2002<sup>10</sup> while the term was coined in 2009.<sup>11</sup> The PISA is highly efficient way of making self-assembled architectures of block copolymers and it can tolerate very high concentrations of block copolymers (as high as 50 wt%) that is amenable to scalability. The PISA method is been mainly explored for radical polymerization

processes such as ATRP, RAFT, nitroxide mediated polymerization (NMP),<sup>12</sup> etc. of vinyl monomers and numerous polymer morphologies were produced. Apart from radical based polymerization of vinyl monomers, the ring opening metathesis polymerization is also employed in PISA process (known as ROMPISA).<sup>13</sup> There has been significant advancement in PISA optimization by employing various initiating conditions such as thermal initiation, sonication, photoinitiation, microwave irradiation, enzymatic initiation, etc., and wide variety of solvents such as water,<sup>14</sup> n-alkanes,<sup>15</sup> ethanol,<sup>16</sup> etc. were used. With the help of PISA, various stimuli responsive nano objects such as thermoresponsive,<sup>17</sup> pH responsive,<sup>18</sup> photo responsive,<sup>19</sup> etc. were synthesized. Due the advancements in PISA it has been used for wide variety of applications including biomedical applications via in-situ encapsulation of drugs.<sup>20</sup>

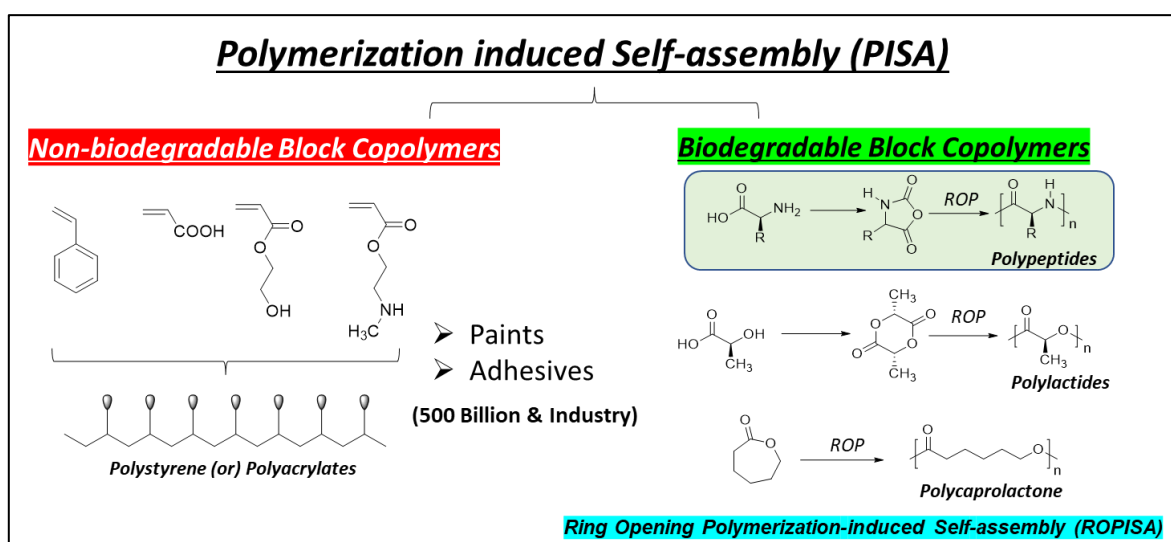
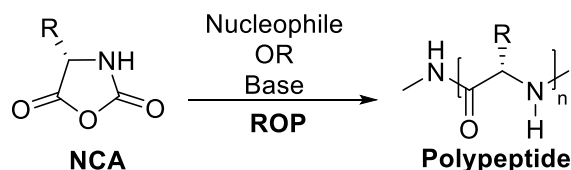


**Figure 1.2:** Monomers utilized in PISA to make biodegradable or non-biodegradable polymers

Although, PISA is extremely beneficial process for block copolymer self-assembly it suffers from a major drawback of non-biodegradable nature of resultant polymers and utility of petroleum-based vinyl monomers.<sup>21</sup> To overcome the biodegradability issue, the ring opening polymerization (ROP) of caprolactone, lactide or N-carboxy anhydride (NCA) monomers can be coupled with PISA to make biodegradable block copolymers based on polyester or polypeptide backbone (see Figure 1.2). Among them, polypeptides can be a great choice since they are not only biodegradable but they are derived from biobased monomers such as amino acids.

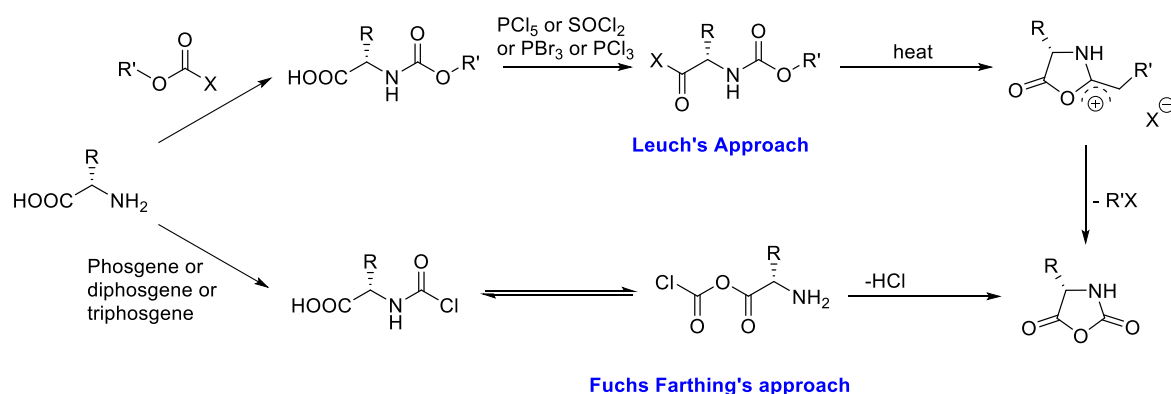
## 1.1. Polypeptides

The polypeptides are the synthetic polymers which are typically synthesized by nucleophile or base initiated ROP of amino acid derived NCA monomers<sup>22</sup> (see scheme 1.1). The ROP of NCA utilizes simple reagents, benign conditions and polypeptides with very high molecular weight (up to 87 MDa) can be easily synthesized in high yields (> 90 %) and in large quantities (gram scale) without affecting chirality of amino acid.<sup>22</sup>



**Scheme 1.1.** Schematic representation of NCA polymerization

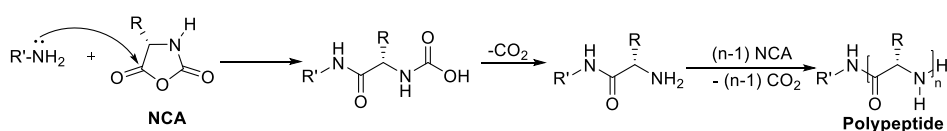
The NCA monomer is synthesized from amino acid by two different approaches as shown in scheme 1.2. The first approach is two-step process developed by Leuch and hence known as Leuch's method.<sup>23</sup> Leuch's method begins with the treatment of amino acids with alkoxy chloroformates to yield N-carbamoyl amino acid intermediate and it is followed by reaction with any of the halogenating agents such as  $\text{PCl}_3$ ,  $\text{SOCl}_2$ , etc to afford NCAs. The second approach is single step process known as Fuchs-Farthing method, which involves carbonylation and in-situ cyclization of amino acids to get NCA by phosgenation. Due to the simplicity and ease of NCA isolation, the Fuchs-Farthing method is the most widely employed procedure for synthesis of NCA. Even though, the Fuchs-Farthing method is quite simple for synthesis of NCA monomer, it produces HCl as side product that has to be completely removed to afford pure NCA. This is because presence of HCl impurity in NCA monomer can either lead to termination of growing polymer chain or chloride ion-initiated ROP of NCA as a result, HCl quenchers such as  $\alpha$ -pinene or propylene oxide were developed.



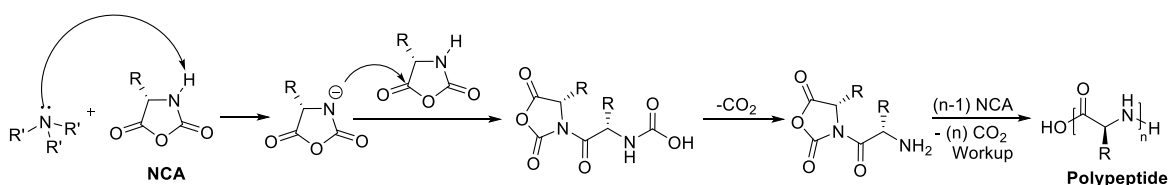
**Scheme 1.2.** Schematic representation of NCA synthesis

The NCA ROP is conventionally initiated by nucleophiles or bases such as primary amines, alkoxides, tertiary amines, etc. The NCA ROP mostly follows two common pathways such as NAM (normal amine mechanism) and AMM (activated monomer mechanism) (see Scheme 1.3) <sup>24</sup>. In case of NAM, the nucleophile attacks anhydride carbonyl of NCA which lead to opening of highly strained NCA ring to yield unstable carbamic acid intermediate that undergoes decarboxylation to generate amine terminated species that attacks next incoming NCA and this process continues to obtain polypeptide. In NAM process, the rate of initiation is higher than rate of propagation that leads to better control over polymerization process and hence usually in absence of side reactions, the polypeptides having expected molecular weight can be synthesized in NAM process. On the other hand, in case of AMM, NCA ring NH is deprotonated by base to yield NCA anion and that acts as nucleophile to open other NCA monomer and polymerization continues to get polypeptide. The AMM process is usually uncontrolled as a result of slow initiation and faster propagation and that leads to synthesis of polypeptides with higher dispersity ( $\bar{D}$ ) and having higher molecular weights than expected.

(a) Normal Amine Mechanism (NAM)



(a) Activated Monomer Mechanism (AMM)



**Scheme 1.3.** Scheme representation (a) Normal amine mechanism for ROP of NCA  
(b) Activated monomer mechanism for ROP of NCA

In common practice, these two pathways can operate simultaneously and often compete with each other. The extent of operating pathway is decided by the nucleophilicity or basicity of initiators. The more basic initiator will lead to predominant AMM pathway while more nucleophilic initiator leads to predominant NAM pathway. Primary amines are preferred initiators for NCA ROP since they are more nucleophilic which lead to NCA ROP predominantly via NAM pathway. However, due to slight basicity of primary amines, AMM pathway is also operated simultaneously to some extent, especially for preparation of very high molecular weight polypeptides (high monomer to initiator, M/I ratio) and hence there was need of catalysts or novel initiators for controlled NCA ROP. The controlled ROP of NCA for synthesis of polypeptide block copolymer was first time shown by Deming by employing transition metal catalysis.<sup>25</sup> Since then, publications on controlled living ROP of NCAs have flooded in the polypeptide literature,<sup>26</sup> making it easier to synthesise polypeptide and hybrid materials with a variety of topologies, including block copolymers, graft copolymers, random copolymers, and star-shaped polymers. These outstanding developments in NCA ROP chemistry have made it possible to build a variety of supramolecular structures based on polypeptides, including hydrogels, micelles, vesicles, and hybrid nanoparticles. In the last two decades, there has been more attention towards developing synthetic polypeptides from NCA ROP with enhanced polymerization kinetics and controlled living polymerization. Some of these developments include developing novel catalysts for conventional primary amine-initiated ROP of NCA, using innovative polymerization conditions such as high vacuum and nitrogen flow, and using different initiators other than conventional primary amines such as HMDS<sup>26</sup>, PhS-SiMe<sub>3</sub> or PhS-SnMe<sub>3</sub><sup>27</sup>, and LiHMDS.<sup>28</sup> In addition to these outrageous initiators, accelerated kinetics of NCA ROP was observed for novel initiator molecules containing both tertiary amine (or secondary amine) and primary amine functionality in a single chemical entity. These so-called "allied amines" are excellent initiators for ROP of NCA owing to their fast kinetics and good control over ROP. Recently, apart from these outrageous initiators, there has been a significant advancement in the development of catalysts for greatly accelerated controlled ROP of NCA by alcohols<sup>29</sup> as initiators. In most of the reported NCA ROP was carried out in organic solvents

such as DMF, chloroform, dichloromethane, THF<sup>30</sup>, etc. However, there has been few recent reports on NCA ROP in chloroform (or dichloromethane) emulsion. These recent reports gave a hint that NCA polymerization can tolerate moisture and it led to development of NCA polymerization in water.

## **1.2. Ring opening polymerization induced self-assembly (ROPISA) of polypeptides**

Due to recent advancements in polypeptide area, several polypeptide block copolymer architectures were synthesized by employing conditions mentioned above and then they were self-assembled in post polymerization process for biomedical applications. However, there are only handful of reports wherein ROP of NCA is combined with PISA process to make polypeptide nanoparticles and the process is called as ring opening polymerization induced self-assembly (ROPISA). The ROPISA for polypeptide synthesis was demonstrated by Jinhui Jiang, et. al. wherein they polymerized phenyl alanine NCA in THF using PEG amine initiator to prepared polypeptide vesicles in THF<sup>30</sup>. The process was carried out in open air, in cold conditions to yield self-assembled polypeptide at concentration as high as 20 wt%. Subsequently, Giuseppe Battaglia and co-workers reported the polymerization of insitu thermally generated methionine NCA using PEG-amine initiator under ROPISA conditions in dimethyl sulfoxide (DMSO)<sup>31</sup>. In their report, they prepared several oxidation responsive polypeptide nano-objects of various morphologies ranging from worm, micelles to vesicles. Although, in these two reports ROPISA of NCA monomer is described but the process is carried out in organic solvents which makes it difficult to employ for biomedical applications. However, Colin Bonduelle and co-worker came up with a remarkable strategy of doing NCA polymerization in water under ROPISA conditions<sup>32,33</sup>. The water-soluble PEG amine was used as an initiator for polymerization of benzyl glutamate NCA under ROPISA conditions to produce emulsion of PEG-*b*-benzyl glutamate that exhibited worm like morphology. In this aqueous ROPISA process the water-soluble PEG amine initiates the polymerization of NCA that initially results in the formation of short amphiphilic oligomers which subsequently self-assembles and encapsulates the unreacted NCA molecules in their hydrophobic cavity and protects these NCA molecules from hydrolysis. These self-assembled oligomeric amphiphilic chains continue to grow by consuming all NCA monomer trapped inside their cavity to form polypeptide emulsion at the end. In



addition to benzyl glutamate NCA, similar strategy was employed for lysine and leucine based NCA monomers. Aqueous ROPISA of NCA is recently started area and it would be even better if photo crosslinking is employed on resultant polypeptide emulsions since the photo crosslinked polypeptide emulsions would be even more stable and amenable to various morphologies.

### 1.3. Photo Crosslinking

Photo crosslinking is a process that involves the use of light to initiate the formation of covalent bonds between molecules, leading to the formation of a three-dimensional network. It is a powerful tool for creating polymer networks because it permits the creation of strong bonds between polymer chains even when reaction conditions are mild, such as ambient temperature and pressure <sup>34</sup>. Photo crosslinking is advantageous to alternative crosslinking techniques in several ways <sup>35</sup>. Typically, it can be done quickly, cheaply, under strict control, and at room temperature using solvent-free technologies. Additionally, there is no need for cross-linking agents, no by-products are produced during the process, and it may be utilized to insert functional groups into the polymer network. It has excellent spatial resolution and extremely high cross-linking rates. <sup>35</sup>Due to its distinct advantages in real-world applications, such as the synthesis of hydrogels, coatings, and adhesives, photo-initiated cross-linking has attracted significant interest on both an economic and environmental level. It has been applied in the biomedical industry to produce biosensors, drug-delivery devices, and tissue-engineered constructs. This technique is widely used in polymer chemistry, material science, and biochemistry fields.

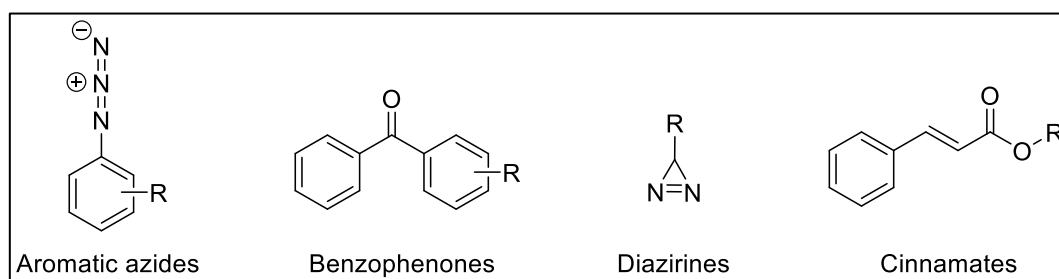


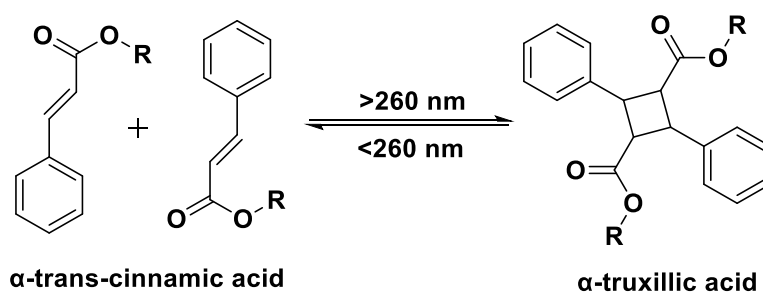
**Figure: 1.3 – Different photo crosslinking groups**

The photo crosslinking in polymers is carried out by attaching photoactivatable small molecules to polymer backbone which can directly crosslink under light

irradiation when exposed to light of a given wavelength. These molecules typically contain a photoactivatable group, such as a benzophenone, diazirines or coumarin moiety, that can undergo a photochemical reaction when exposed to light, leading to the formation of reactive species that can initiate crosslinking. The functional groups that are commonly used for photo crosslinking are given in figure 1.3. Aromatic azides generate nitrene intermediate for crosslinking. Another common moiety is benzophenone<sup>36</sup> which upon irradiation forms highly reactive ketyl radical which undergoes crosslinking and indeed new materials with distinctive features, like shape-memory materials and self-healing polymers, have been produced using this process. Another photo cross linkable molecule is diazirene moiety which upon irradiation releases gaseous nitrogen and generates highly reactive carbene intermediate that undergoes crosslinking by various insertion reactions with neighbouring groups. The photo crosslinking reaction in all these discussed moieties is irreversible however it would be great if the photo crosslinking chemistry is reversible and that is achieved by cinnamoyl group.

#### **1.4. Cinnamoyl group for photo crosslinking**

The cinnamic group has received the most attention among the numerous photo-cross-linkable groups listed above because of its excellent reversible photo-reactivity when exposed to UV light. In accordance with the topochemical principle, a photoreaction can take place between two molecules that have parallel double bonds and an intermolecular double bond distance of less than  $4.2 \text{ \AA}$ <sup>37</sup>. The trans-cinnamic acid crystal structures of the monomorph and polymorph satisfy these requirements, and irradiation of such compounds results in the relevant cycloaddition products. When exposed to UV light, cinnamic groups, whether found in the side chain or the backbone of a polymer, absorb this light which leads to the formation of a reactive species called a triplet excited state.<sup>38,39</sup> The triplet excited state of the cinnamoyl group can react with a neighbouring cinnamoyl group in a process known as a [2+2] photocycloaddition. This reaction involves the formation of a cyclobutane ring between the two cinnamoyl groups<sup>40</sup>. The reaction can be reversed upon irradiation of light of another wavelength.



**Scheme: 1.4** – Cinnamoyl crosslinking: [2+2] cycloaddition

The resulting crosslinked polymer network has enhanced mechanical properties, such as increased strength and toughness, due to the formation of intermolecular crosslinks.<sup>38</sup> Cinnamoyl-based photo crosslinking offers characteristics that make it a desirable choice for creating innovative materials with specialised properties for certain applications, such as coatings, adhesives, and microelectronics. It's important to note that the efficiency of cinnamoyl photo crosslinking depends on a variety of factors, such as the concentration of cinnamoyl groups in the polymer, the wavelength and intensity of the UV light, and the presence of other chemical species that can compete with the cinnamoyl group for reaction with the triplet excited state.

Cinnamic acid photo crosslinking is employed in polypeptides derived from glutamate based NCA monomers. In one of the reports, the cinnamoyl substituted glutamate NCA monomer was synthesized and then polymerized using PEG amine as initiator to yield cinnamoyl substituted amphiphilic polypeptide which was self-assembled and then irradiated with UV light to prepare crosslinked polypeptide nanoparticles.<sup>35</sup> In another report, similar cinnamoyl substituted PEG-polypeptide di-block copolymer was prepared by post polymerization attachment of cinnamoyl group on to polypeptide backbone and subsequently cinnamoyl conjugated amphiphilic polypeptide di-block copolymer was self-assembled and crosslinked by UV irradiation to yield crosslinked polypeptide nanoparticles.<sup>40</sup> Further, after establishing the photo crosslinking technology, the anticancer drug was encapsulated in amphiphilic cinnamoyl substituted di-block copolymer and subsequently it was crosslinked by UV irradiation to prepare crosslinked drug loaded polypeptide nanoparticles which was found to be stable nano assemblies compared to non-crosslinked drug loaded polypeptide nanoparticles.

## 1.5. Aim of the thesis

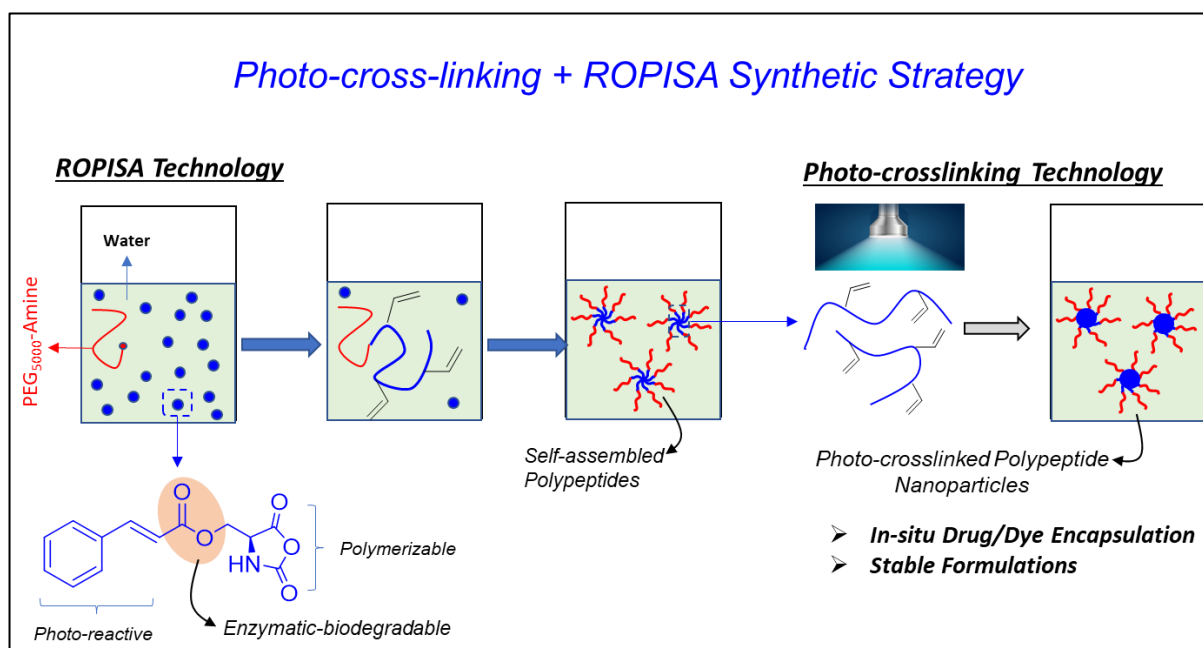


**Figure: 1.4** – Schematic representation of thesis work

Considering this short literature survey, there is quite a lot of scope in developing crosslinked polypeptide nano assemblies. Our lab has interest in making  $\beta$ -sheet polypeptides derived from least explored L-serine amino acid. There has been no report on cinnamoyl substituted serine amino acid or its NCA monomer. Additionally, in our lab serine-based monomers were polymerized under ROPISA conditions and it has been utilized for in situ encapsulation of dye molecules. These findings lead to objective of my thesis, wherein the goal is to make serine-based photo-cross-linked polypeptide nanoparticles via ROPISA methodology. For this purpose, we decided to make cinnamoyl substituted NCA monomer and initially optimize its polymerization under conventional NCA ROP conditions and then under ROPISA conditions. At last, we want to insitu encapsulate dye molecules during ROPISA process of these cinnamoyl substituted NCA monomer and then crosslink these dye loaded polypeptide emulsions.

## 2. Experimental section

### 2.1. Materials

Cinnamoyl chloride,  $\epsilon$ -CBz L-lysine, Nile Red, Rhodamine B, Chloroform-d, Dimethyl sulfoxide-d<sub>6</sub> and Deuterium oxide were purchased from Sigma Aldrich. L-serine, trifluoroacetic acid, diethyl ether, sodium sulphate (anhydrous), sodium bicarbonate, propylene oxide, triphosgene and methanol were purchased from local sellers and used directly. Prior to use, chloroform was refluxed over P<sub>2</sub>O<sub>5</sub> and then distilled. THF and hexane were directly used after distillation. In order to conduct photophysical and morphological experiments, milli-Q water and HPLC grade DMSO were utilised.

### 2.2. Methods

Bruker/Jeol 400 MHz spectrometers were used to record the <sup>1</sup>H and <sup>13</sup>C NMR spectra. On Bruker alpha-E, attenuated total reflectance-Fourier transform infrared (ATR-FTIR) spectra were recorded. GPC was carried out with Viscotek VE 3580 RI detector, Viscotek VE 1122 pump and two size exclusion columns using polystyrene standards. DLS experiments were carried out using the Malven Nano ZS-90 system. Shimadzu UV1900 spectrophotometer was used for absorbance measurements. The Fluorolog HORIBA JOBIN VYON fluorescence spectrophotometer was used to record fluorescence spectra. For HR-TEM analysis, samples were drop casted on copper TEM grids and imaging was performed using Jeol JEM2200FS 200 KeV systems. For AFM analysis, samples were drop casted on a silicon wafer and the AFM imaging was performed using Agilent instruments.

### 2.3. Synthesis

#### 2.3.1. Cinnamoyl serine (C1)

To a solution of TFA (20 mL), L-serine hydrochloride (4 g, 38.06 mmol) was added in portion and was kept for stirring at 4 °C for 10 min and at 25 °C for 5 min. Cinnamoyl chloride (8.2 mL, 57.09 mmol) was added to the reaction mixture and it was kept stirring overnight in N<sub>2</sub> atmosphere. In order to precipitate the reaction product, 60 mL of diethyl ether (Et<sub>2</sub>O) was added, and the mixture was stirred again for 15 minutes. The resulting mixture was vacuum filtered and was washed with Ethyl acetate (EtOAc) (120 mL) and acetone (40 mL). The product was purified by dissolving the residue in methanol and precipitating again in Et<sub>2</sub>O. The mixture was let to stand at -20 °C for

the entire night. It was filtered, washed with acetone and dried under high vacuum to yield cinnamoyl serine (**C1**) as pure crystalline solid. Yield = 9.8 g (95%).

$^1\text{H}$  NMR (400 MHz, DMSO- $d_6$ , TMS)  $\delta$  ppm: 4.38 (t, 1H), 4.51 – 4.60 (m, 2H), 6.58 (d, 1H), 7.43 - 7.47 (m, 3H), 7.68 - 7.73 (m, 2H), 7.81 (d, 1H).  $^{13}\text{C}$  NMR (101 MHz,  $\text{CDCl}_3$ , TMS)  $\delta$  ppm: 51.2, 62.9, 117.5, 128.2, 129.7, 131.5, 134.6, 145.4.

### 2.3.2. Cinnamoyl L-Serine NCA (**M1**)

To a round-bottom flask containing the solvent THF (40 mL), cinnamoyl L-serine (4 g, 7.37 mmol) was added followed by propylene oxide (4.97 mL, 36.83 mmol). It was stirred for a few minutes. To this turbid solution, triphosgene (2.19 g, 3.68 mmol) was added subsequently. The reaction mixture became completely clear within minutes. It was stirred for 2 h. The mixture precipitated after being filtered into dry hexane (120 mL). The mixture was let to stand at  $-20\text{ }^\circ\text{C}$  for the entire night and it produced pure crystalline NCA after being filtered, washed with dry hexane, and dried under high vacuum. Yield = 3.2 g (83.2%).

$^1\text{H}$  NMR (400 MHz,  $\text{CDCl}_3$ , TMS)  $\delta$  ppm: 4.5 (dd, 1H), 4.78 – 4.79 (m, 1H), 4.92 (dd, 1H), 6.48 (d, 1H), 7.38 - 7.49 (m, 4H), 7.55 - 7.58 (m, 2H), 7.79 (d, 1H).  $^{13}\text{C}$  NMR (101 MHz,  $\text{CDCl}_3$ , TMS)  $\delta$  ppm: 58, 62, 114, 115, 118, 131, 133, 149, 155. ATR-FTIR ( $\text{cm}^{-1}$ ): 1497, 1577, 1635, 1707, 1781, 1857.

### 2.3.3. $\gamma$ -benzyl L-Glutamate NCA (**M2**)

$\gamma$ -benzyl L-Glutamate (4 g, 16.86 mmol) was added to a round-bottom flask containing the solvent THF (60 mL). propylene oxide (4.55 mL, 67.44 mmol) was added to it followed by triphosgene (2.5 g, 8.43 mmol). It was kept stirring for 2 h in  $\text{N}_2$  atmosphere, where the reaction mixture became completely clear. After completion of the reaction 30 mL  $\text{H}_2\text{O}$  was added to the reaction mixture and it was stirred for exactly 1 min. The mixture was extracted by EtOAc (2x50 mL), the organic layer with brine (1x30 mL), dried over  $\text{Na}_2\text{SO}_4$  and the EtOAc was removed under reduced pressure. The product was dissolved in THF (40 mL) and filtered out. Dry hexane (160 mL) was added to the above filtrate to precipitate out the product. The mixture was allowed to stand for overnight at  $-20\text{ }^\circ\text{C}$ , filtered, washed with dry hexane, and dried under high vacuum to yield pure crystalline NCA. Yield = 3.2 g (72%).

$^1\text{H}$  NMR (400 MHz,  $\text{CDCl}_3$ , TMS)  $\delta$  ppm: 2.07 – 2.16 (m, 1H), 2.24 – 2.32 (m, 1H), 2.59 (t, 2H), 4.37 (t, 1H), 5.14 (s, 2H), 7.32 - 7.41 (m, 5H).  $^{13}\text{C}$  NMR (101 MHz,  $\text{CDCl}_3$ , TMS)  $\delta$  ppm: 27, 30, 57.1, 67.3, 128.5, 128.7, 128.9, 135.3, 151.9, 169.5, 172.5. ATR-FTIR ( $\text{cm}^{-1}$ ): 1498, 1731, 1779, 1857.

#### 2.3.4. CBz-lysine NCA (M3)

A white crystalline solid was obtained from CBz-L-lysine hydrochloride (4 g, 14.27 mmol), propylene oxide (9.64 mL, 142.69 mmol) and triphosgene (2.12 g, 7.14 mmol) by using the same procedure as that for  $\gamma$ -benzyl L-Glutamate NCA monomer. Please note that the reaction mixture was stirred for 3 h. Yield = 3.7 g (85%).

$^1\text{H}$  NMR (400 MHz,  $\text{CDCl}_3$ , TMS)  $\delta$  ppm: 1.37 – 1.59 (m, 4H), 1.74 (s, 2H), 3.14 – 3.27 (m, 2H), 4.25 – 4.28 (m, 1H), 5.07 – 5.13 (m, 2H), 7.30 - 7.39 (m, 5H).  $^{13}\text{C}$  NMR (100 MHz,  $\text{CDCl}_3$ , TMS)  $\delta$  ppm: 21, 29.1, 30.6, 57.4, 67, 128, 128.1, 128.2, 128.6, 136.2, 152.2, 157, 169.8. ATR-FTIR ( $\text{cm}^{-1}$ ): 1529, 1689, 1771, 1806, 1856.

#### 2.3.5. Polymer synthesis

##### 2.3.5.1. Di-block copolymers: PEG-b-P(Cser) $_n$

Detailed polymerization procedure is described for the synthesis of PEG-b-P(Cser) $_{25}$ , initiated by PEG amine in dry  $\text{CHCl}_3$  using NHC catalyst.

A Schlenk tube with both the initiator, PEG amine (200 mg, 0.04 mmol) and catalyst, NHC (5.86 mg, 0.016 mmol) was taken and dried under vacuum. Dry chloroform (10 mL) was added under nitrogen environment. The serine monomer, **M1** (266 mg, 1 mmol) was added and the reaction mixture was stirred overnight at 25 °C. The FTIR was checked, after the confirmation of disappearance of monomer (anhydride) peaks, under reduced pressure, the chloroform was removed, and methanol was added to cause the polymer to precipitate (40 mL). The suspension was poured into a centrifuge tube and spun for 15 minutes at 4000 rpm. The pellet was dried under high vacuum after the supernatant was discarded to produce PEG-b-P(Cser) as a white solid. Yield=230 mg (55%).

$^1\text{H}$  NMR (400 MHz,  $\text{CDCl}_3$ , TMS)  $\delta$  ppm: 3.7 (s, 452H), 4.3 – 4.7 (m, 60H), 4.8 – 5.0 (m, 26H), 6.2 (d, 26H), 7.1 - 7.5 (m, 210H), 7.6 (d, 27H). ATR-FTIR ( $\text{cm}^{-1}$ ): 1495, 1557, 1577, 1635, 1664, 1715.

For polymerization at M/I = 100, the same procedure as that for M/I = 25 was followed. Dry CHCl<sub>3</sub> (10 mL), PEG amine (100 mg, 0.02 mmol), serine monomer (**M1**) (522 mg, 2 mmol) and NHC catalyst (2.93 mg, 0.008 mmol) were used for the polymerization. Yield=528 mg (99%).

<sup>1</sup>H NMR (400 MHz, CDCl<sub>3</sub>, TMS) δ ppm: 3.7 (s, 452H), 4.5 (dd, 194H), 4.9 – 5.0 (m, 101H), 6.2 (d, 101H), 7.1 - 7.5 (m, 598H), 7.6 (d, 102H).

### 2.3.5.2. Tri-block copolymer synthesis

#### PEG-b-P(Cser)<sub>25</sub>-b-P(BnGlu)<sub>100</sub> (**P3**)

Detailed block polymerization procedure is described for the synthesis of PEG-b-P(Cser)<sub>25</sub>-b-P(BnGlu)<sub>100</sub> initiated by PEG amine in dry CHCl<sub>3</sub> using NHC catalyst.

A Schlenk tube with both the initiator, PEG amine (100 mg, 0.02 mmol) and catalyst, NHC (2.93 mg, 0.008 mmol) was taken and it was dried under vacuum. Dry chloroform (10 mL) was added under nitrogen environment. The serine monomer, **M1** (130 mg, 0.5 mmol) was added and the reaction mixture was stirred for overnight at 25 °C with constant nitrogen flow. The FTIR was checked, after the confirmation of disappearance of monomer (anhydride) peaks, 200 µL of reaction mixture was taken as aliquot for further studies. Subsequently the next monomer i.e., benzyl glutamate NCA, **M2** (516 mg, 1.96 mmol) was added and the reaction mixture was stirred for 2 h at 25 °. The FTIR was checked, after the confirmation of disappearance of monomer (anhydride) peaks, under reduced pressure, the chloroform was removed, and methanol was added to cause the polymer to precipitate (40 mL). The suspension was poured into a centrifuge tube and spun for 15 minutes at 4000 rpm to get a light-yellow solid of PEG-b-P(Cser)<sub>25</sub>-b-P(BnGlu)<sub>100</sub>. Yield = 602 mg (94 %).

<sup>1</sup>H NMR (400 MHz, CDCl<sub>3</sub>, TMS) δ ppm: 1.8 – 2.0 (m, 113H), 2.0 – 2.2 (m, 105H), 2.3 – 2.5 (m, 211H), 3.7 (s, 452H), 4.6 (s, 110H), 6.3 (d, 25H), 7.6 (d, 26H). ATR-FTIR (cm<sup>-1</sup>): 1497, 1546, 1652, 1729.

#### PEG-b-P(Cser)<sub>25</sub>-b-P(CbzLys)<sub>100</sub> (**P4**)

The procedure similar to that for PEG-b-P(Cser)<sub>25</sub>-b-P(BnGlu)<sub>100</sub> is employed.



PEG amine (100 mg, 0.02 mmol), NHC (2.93 mg, 0.008 mmol), serine monomer (**M1**) (130 mg, 0.5 mmol) CBz-Lysine monomer (**M3**) (600 mg, 1.96 mmol) and chloroform (10 mL) were used. Yield = 614 mg (85 %).

$^1\text{H}$  NMR (400 MHz,  $\text{CDCl}_3$ , TMS)  $\delta$  ppm: 1.1 – 1.7 (m, 433H), 1.5 – 1.8 (m, 216H), 2.1 (s, 210H), 3.7 (s, 452H), 5.1 (s, 232H), 6.2 (d, 25H). ATR-FTIR ( $\text{cm}^{-1}$ ): 1536, 1647, 1705.

### 2.3.6. ROPISA mediated polymerization

The procedure is explained in detail for  $M/I = 25$ .

50 mM aq.  $\text{NaHCO}_3$  (10 mL) was introduced to a cylindrical polymerization tube, which was then cooled on an ice bath at 4 °C. MeO-PEG<sub>5000</sub>-NH<sub>2</sub> (336 mg, 0.067 mmol) was added to the polymerization tube and it was stirred at 4 °C to get a clear solution. To this solution, serine monomer (**M1**) (438 mg, 1.677 mmol) was added, and the reaction mixture was vigorously stirred in the dark at 4 °C for 8 hours and at 25 °C for 40 hours. At the end of the reaction, the mixture turned into a blue tinted opalescent solution. To monitor the reaction progress by FT-IR, a small aliquot (100  $\mu\text{L}$ ) was taken out and extracted with DCM (200  $\mu\text{L}$ ), and the DCM layer was used for FT-IR measurements. Upon confirmation of consumption of the monomer (disappearance of anhydride peaks), the opalescent reaction mixture was dialyzed against MilliQ water with frequent change of water. 1 mL of the dialyzed solution was lyophilized, and the resulting white fluffy powder was used for  $^1\text{H}$ -NMR, GPC measurements.

$^1\text{H}$  NMR (400 MHz,  $\text{CDCl}_3$  TMS)  $\delta$  ppm: 3.5 (s, 3H), 3.7 (s, 452H), 4.3 – 4.7 (m, 53H), 4.8 – 5.0 (m, 25H), 6.2 (d, 26H), 7.6 (d, 25H). ATR-FTIR ( $\text{cm}^{-1}$ ): 1513, 1552, 1635, 1666, 1717.

For polymerization at  $M/I = 10$ , the same procedure as that for  $M/I = 25$  was followed. 50 mM aq.  $\text{NaHCO}_3$  (5 mL), MeO-PEG<sub>5000</sub>-NH<sub>2</sub> (244 mg, 0.049 mmol) and serine monomer (**M1**) (127 mg, 0.488 mmol) were used for the polymerization.

$^1\text{H}$  NMR (400 MHz,  $\text{CDCl}_3$ , TMS)  $\delta$  ppm: 3.7 (s, 452H), 4.3 – 4.7 (m, 21H), 4.8 – 5.0 (m, 11H), 6.2 (d, 12H), 7.1 - 7.5 (m, 60H), 7.6 (d, 13H). ATR-FTIR ( $\text{cm}^{-1}$ ): 1466, 1515, 1637, 1719.

For polymerization at M/I = 50, the same procedure as that for M/I = 25 was followed. 50 mM aq. NaHCO<sub>3</sub> (5 mL), MeO-PEG<sub>5000</sub>-NH<sub>2</sub> (110 mg, 0.22 mmol) and serine monomer (**M1**) (288.3 mg, 1.102 mmol) were used for the polymerization. The reaction mixture was quite turbid, making it difficult to isolate the polymer; hence it was not characterised.

For polymerization at M/I = 100, the same procedure as that for M/I = 25 was followed. 50 mM aq. NaHCO<sub>3</sub> (5 mL), MeO-PEG<sub>5000</sub>-NH<sub>2</sub> (65.5 mg, 0.013 mmol) and serine monomer (**M1**) (342 mg, 1.31 mmol) were used for the polymerization. The reaction mixture was thickly turbid, making it difficult to isolate the polymer; hence it was not characterised.

### 2.3.7. In-situ encapsulation of Dyes via ROPISA

The procedure for encapsulating Rhodamine B is described. 50 mM aq. NaHCO<sub>3</sub> (5 mL) was introduced to a cylindrical polymerization tube, which was then cooled on an ice bath at 4 °C. MeO-PEG<sub>5000</sub>-NH<sub>2</sub> (168 mg, 0.033 mmol) was added to the polymerization tube and it was stirred at 4 °C to get a clear solution. Rhodamine B (17 mg) and serine monomer (**M1**) (209 mg, 0.835 mmol) were then added, and the polymerization mixture was vigorously stirred in the dark for 8 hours at 4 °C and subsequently for 40 hours at 25 °C. At the end of 48 h, the resultant-coloured solution was filtered through Whatman filter paper to get rid of unencapsulated insoluble Rhodamine B particles. 1 mL of the resultant filtered solution was diluted with MiliQ water (2 mL) and this solution was dialyzed against MiliQ water in dark for 48 h. The filtered and dialyzed solution was stored at 4 °C. A small fraction of this dialyzed solution (500 µL) was lyophilized to get solid powder composed of polymer and encapsulated Rhodamine B. It was dissolved in DMSO and this solution was used to calculate DLC (dye loading content).

Weight of encapsulated dye in the resultant solution was determined by measuring absorbance at absorption maxima of dialysed solutions. The DLC were determined by using the following equation:

$$\text{DLC} = [\text{weight of encapsulated dye/weight of polymer}] \times 100$$

Nile Red ( $\epsilon = 19600 \text{ L.M}^{-1}.\text{cm}^{-1}$  at 552 nm) and Rhodamine B ( $\epsilon = 116000 \text{ L.M}^{-1}.\text{cm}^{-1}$  in DMSO and  $111500 \text{ L.M}^{-1}.\text{cm}^{-1}$  in water at 553 nm).

## 2.4. CMC measurements

Using hydrophobic pyrene as the probe, the reported approach was used to evaluate the CMC of the block copolymer PEG-b-P(Cser)<sub>25</sub> in aqueous solution. 100  $\mu$ L of 18  $\mu$ M pyrene in acetone was added to the vials and they were kept overnight to evaporate acetone. Varying concentration of polymer was prepared and added to pyrene-coated vials. It was sonicated for 3 hours continuously and equilibrated overnight. It was again sonicated for half an hour and finally, these vials were purged with nitrogen. Fluorescence of the resulting solution was measured by fluorescence spectrophotometer using slit width of 2 nm and excitation wavelength of 337 nm. The linear relationship between the concentration of surfactant and the ratio of its emission intensities at the peaks I (372 nm) and III (382 nm) is the basis for the CMC determination.

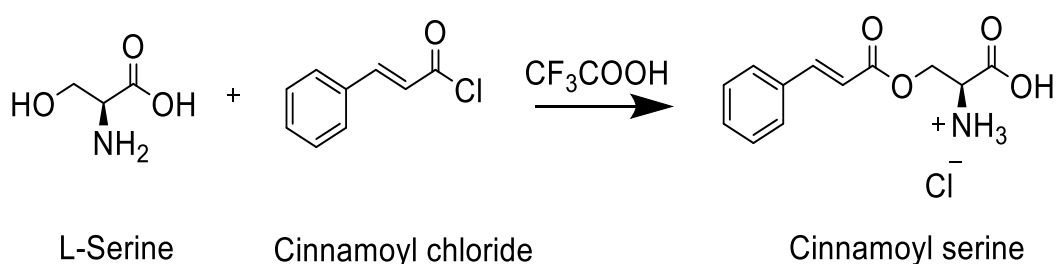
## 2.5. Photo crosslinking strategy.

The photo dimerization of the cinnamoyl group was carried out under UV light. The ROPISA polymer samples of varying concentrations were taken in a Petri dish (kept in an ice bowl) and subjected to UV illumination using the UV lamp of  $\lambda = 264$  nm. In order to track the crosslinking kinetics of the polymer, a small amount of the sample solution was taken from the irradiated sample at periodic intervals and subjected to UV-vis absorption measurements. The absorption peak at 285 nm was monitored to study the kinetics of the crosslinking.

### 3. Results and Discussion

#### 3.1. Monomer synthesis and characterization

Cinnamoyl substituted serine (**C1**) was synthesized from L-serine and cinnamoyl chloride and the product was precipitated using diethyl ether (Scheme: 3.1). On purification by precipitation, it gave white crystal. The product was characterised using  $^1\text{H}$  and  $^{13}\text{C}$  NMR.



**Scheme:3.1** – Synthesis of cinnamoyl serine (**C1**).

The  $^1\text{H}$  NMR spectrum (Figure: 3.1.a) shows two doublet peaks at 6.5 ppm and 7.8 ppm corresponding to the two protons of the trans double bond of the cinnamoyl group while, the  $^{13}\text{C}$  NMR spectrum (Figure 3.1.b) shows peaks at 117 ppm and 145 ppm corresponding to the two carbons of the same double bond, confirming the formation of the desired amino acid.

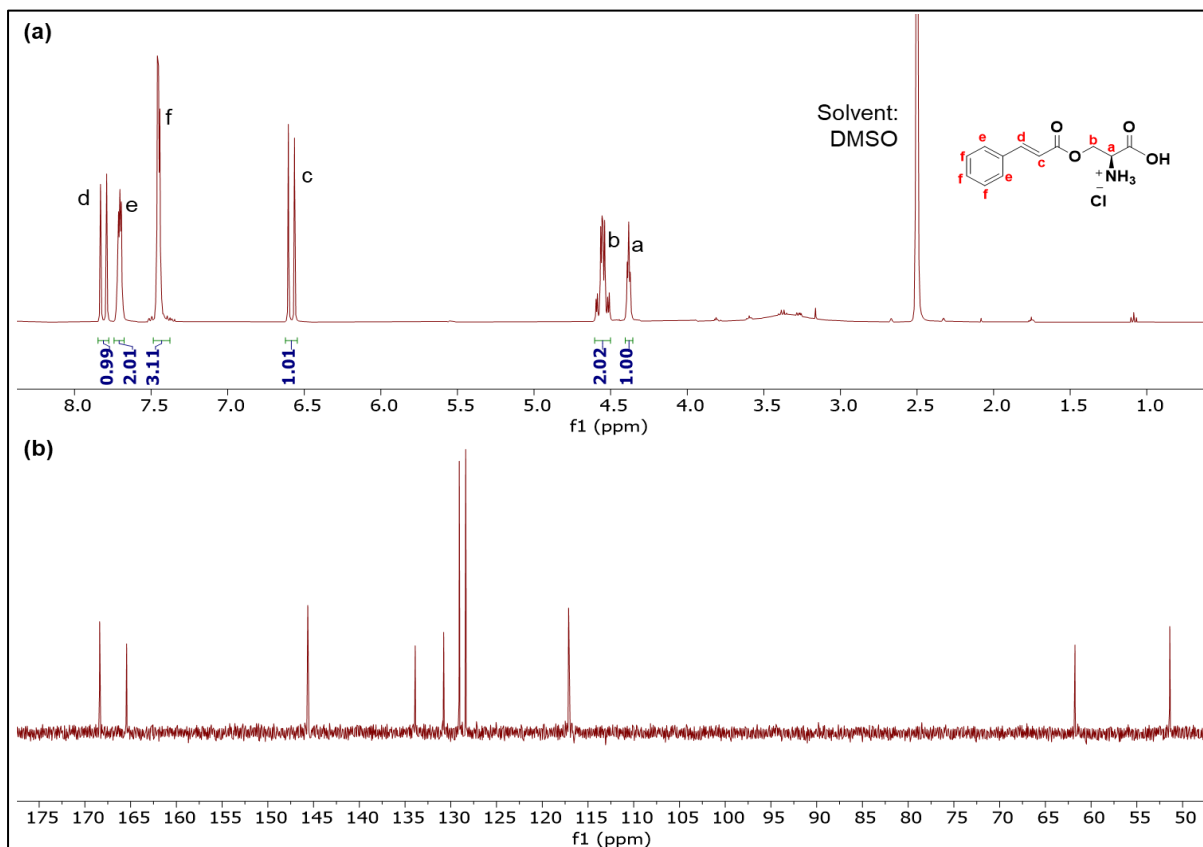
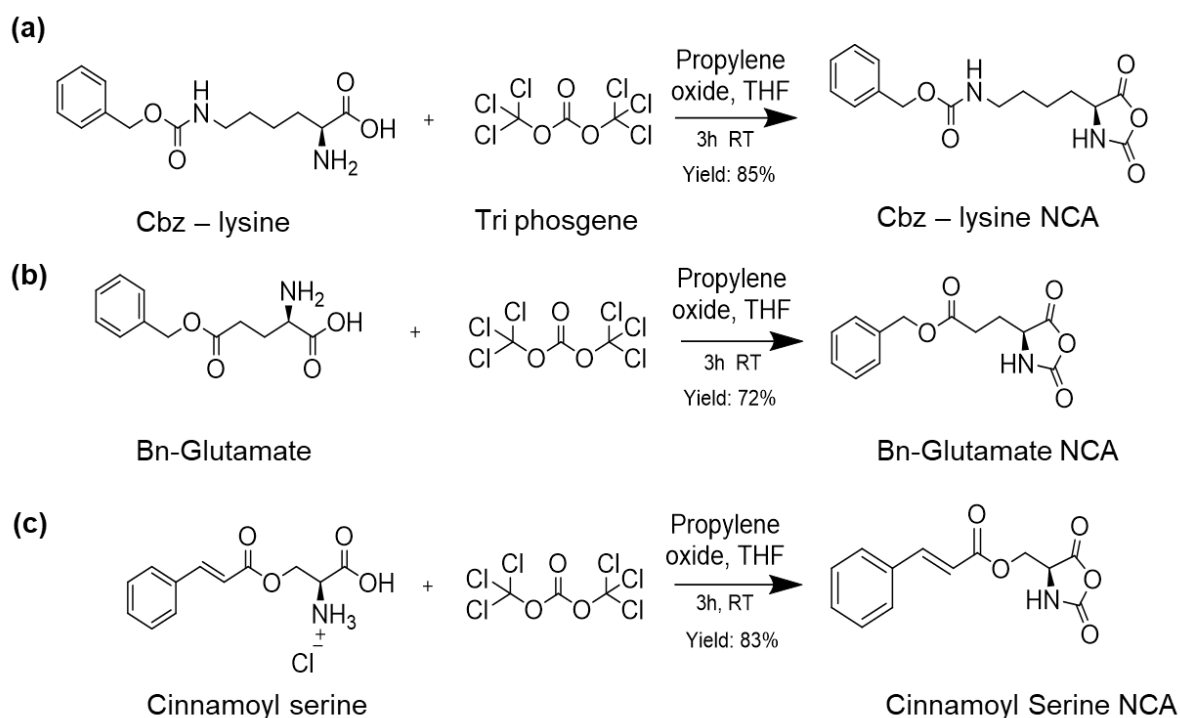


**Figure: 3.1** – (a)  $^1\text{H}$  NMR (b)  $^{13}\text{C}$  NMR of Cinnamoyl L-Serine(**C1**) in  $\text{DMSO}-d_6$

The monomer, cinnamoyl serine NCA (**M1**) was synthesized by the moisture-tolerant route which brilliantly eliminated the need to use dry solvent and inert conditions for NCA synthesis (Scheme: 3.2). Triphosgene was used for the NCA formation and propylene oxide to quench HCl (HCl can cause acid-catalysed decomposition of NCA and also termination of the polymerization process under moist conditions) which is produced during the course of the reaction. The formation of the monomer and its purity were confirmed using  $^1\text{H}$  NMR and FTIR. The peaks in FTIR plot (Figure: 3.2) corresponding to the  $\text{HC}-\text{C}=\text{O}$  and  $\text{HN}-\text{C}=\text{O}$  stretching frequency ( $1851\text{ cm}^{-1}$  and  $1777\text{ cm}^{-1}$  respectively) in NCA confirm the formation of monomer. In the similar manner, NCA monomers of CBz lysine and benzyl glutamate were also synthesized and characterized.



**Scheme: 3.2** – Synthesis of monomer, NCA (a) CBz-lysine NCA(**M3**). (b)  $\gamma$ -benzyl Glutamate NCA(**M2**). (c) Cinnamoyl serine NCA(**M1**).

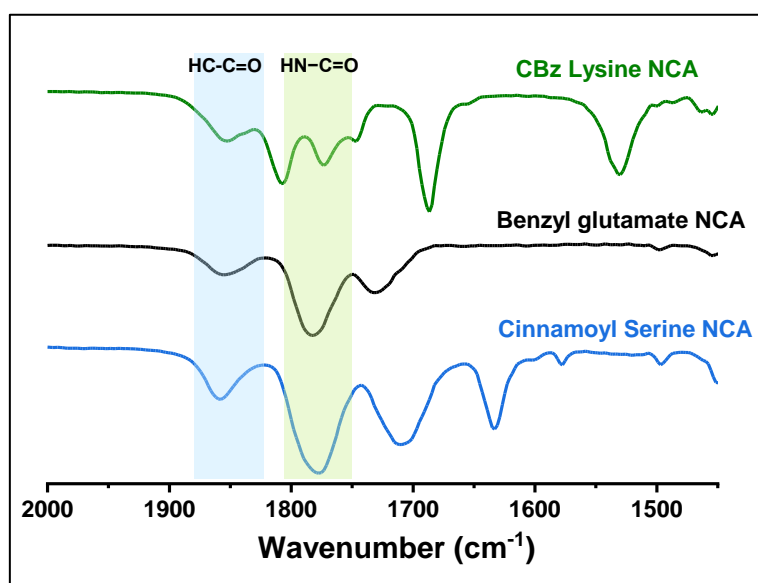


**Figure: 3.2** – FTIR spectrum of monomer, NCA (a) CBz-lysine NCA(**M3**). (b)  $\gamma$ -benzyl Glutamate NCA(**M2**). (c) Cinnamoyl serine NCA(**M1**).

The formation of the product was also confirmed by the  $^1\text{H}$  NMR spectrum, which displayed a downfield peak of ring N-H at 6.8 ppm, 6.6 ppm, and 7.4 ppm for CBz lysine, benzyl glutamate, and cinnamoyl serine NCA's respectively, which gets

de-shielded upon the formation of NCA in comparison to the free amino acid. (Figure: 3.3.a, 3.3.b and 3.3.c respectively).

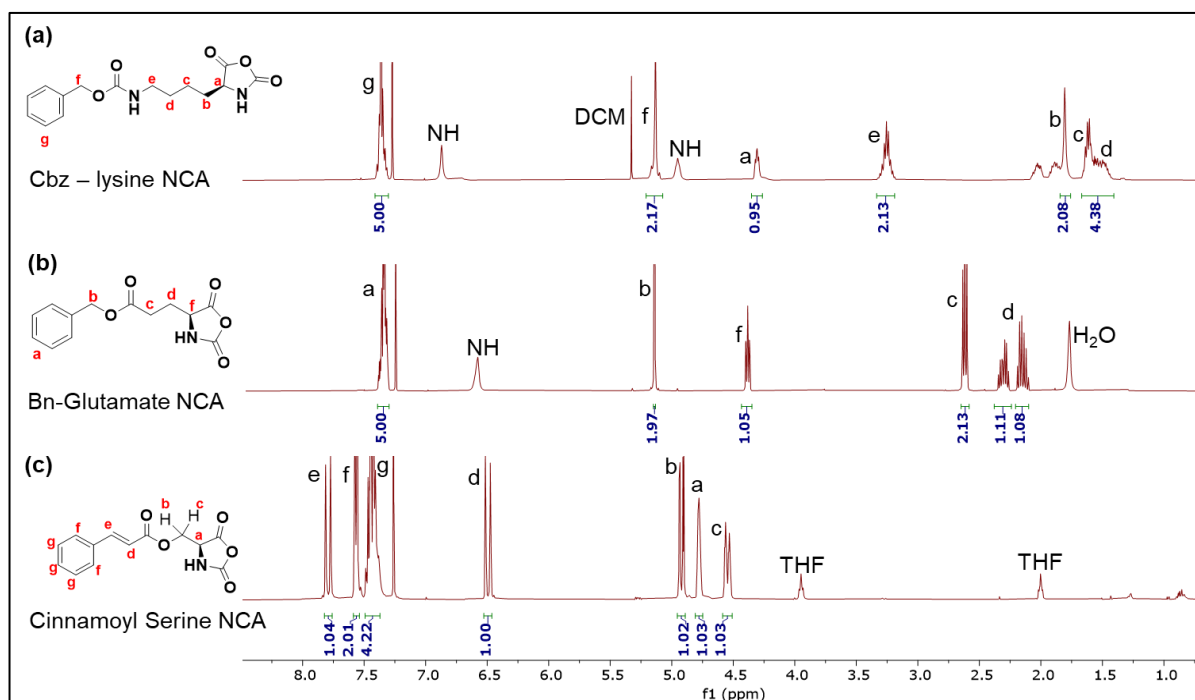
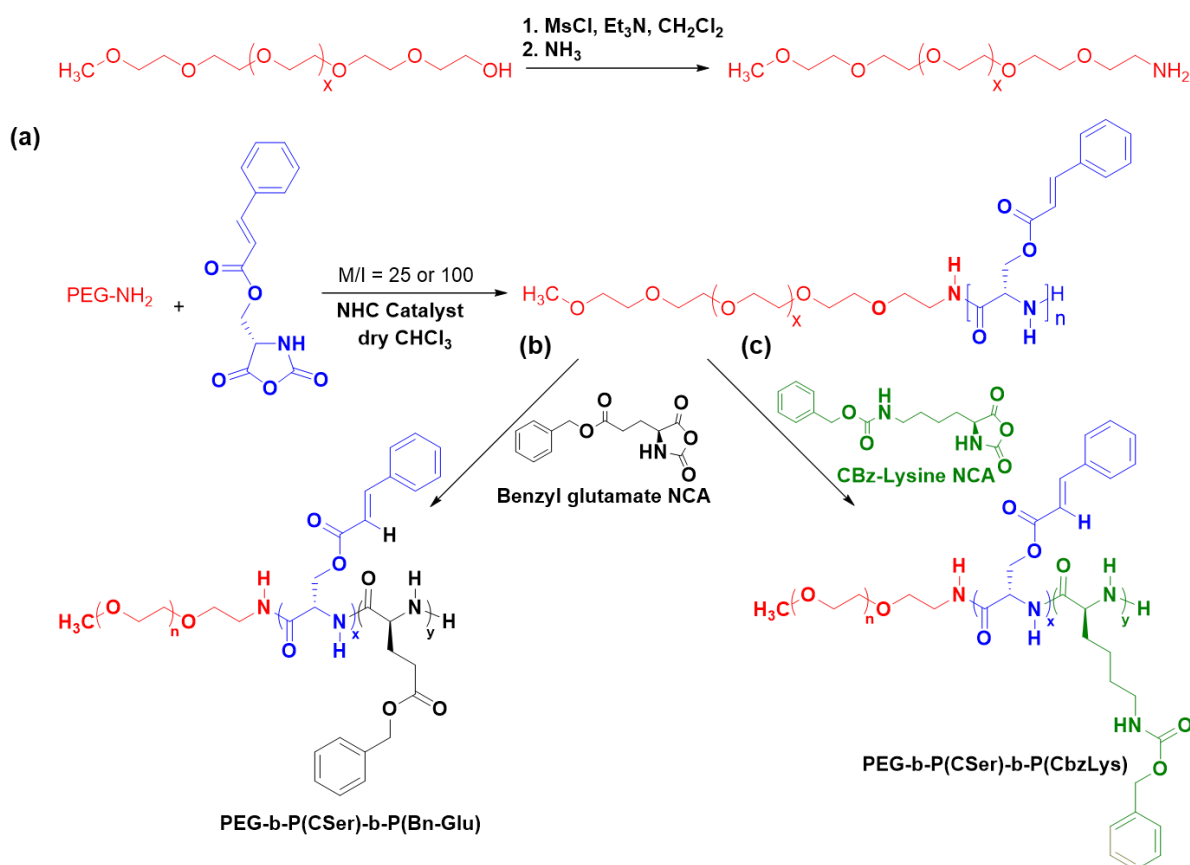


**Figure:3.3** -  $^1\text{H}$  NMR of monomers in  $\text{CDCl}_3$  (a) CBz-lysine NCA(**M3**). (b) benzyl Glutamate NCA (**M2**). (c) Cinnamoyl L-serine NCA (**M1**)

### 3.2. Polymerization in organic solvent (Solution Polymerization)

After making the novel cinnamoyl functionalized serine NCA monomer (**M1**) we went ahead and optimized its polymerization in an organic solvent in the initial studies. Using the formula  $X_n = P \times M/I$  and assuming the P (extent of reaction) to be 100%, we can control the degree of polymerization by varying the monomer to initiator ratio.



**Scheme: 3.3** – synthesis route of (a) Di – block copolymer: PEG-b-P(CSer). (b) Triblock copolymer: PEG-b-P(CSer)-b-P(Bn-Glu) (**P3**). (d) PEG-b-P(CSer)-b-P(CbzLys)(**P4**).

First, we aimed for di-block of cinnamoyl serine NCA using PEG-5K amine as initiator. Polymerization was done in dry chloroform using PEG-5K amine as initiator and N-Heterocyclic Carbene (NHC) as catalyst at 25°C under N<sub>2</sub> atmosphere. M/I ratio of 100 (**P1**) as well 25 (**P2**) was tried. (Scheme 3.3.a)

The completion of polypeptide formation was confirmed by ATR-FTIR. The carbonyl peaks of the monomer for HC-C=O and HN-C=O stretching frequencies (1860 cm<sup>-1</sup> & 1777 cm<sup>-1</sup> respectively) disappear as the polymer is formed and the new peaks corresponding to polypeptide bonds emerges, i.e., peaks corresponding to C=O stretching frequency (amide-I region: 1664 cm<sup>-1</sup>) and the C-N stretching frequency (amide-II region: 1554 cm<sup>-1</sup>) (Figure: 3.4).



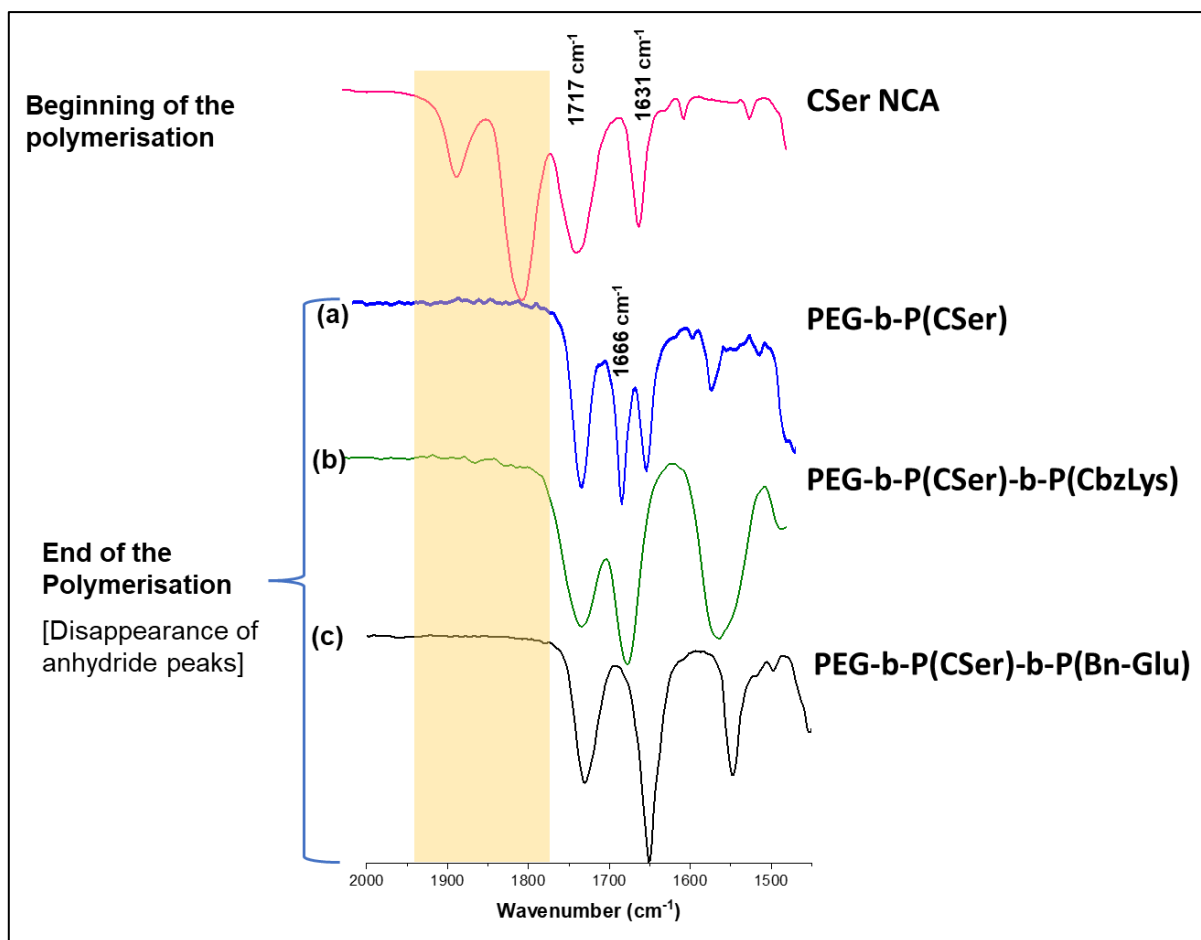


**Figure: 3.4** – FTIR spectra (a) Di – block copolymer: PEG-*b*-P(CSer). (b) Triblock copolymer: PEG-*b*-P(CSer)-*b*-P(CbzLys)(**P4**). (c) PEG-*b*-P(CSer)-*b*-P(Bn-Glu)(**P3**)

The degree of polymerization ( $X_n$ ) was determined using  $^1\text{H}$  NMR. The integration of PEG-chain protons ( $-\text{O}-\text{C}_2\text{H}_4-$ , peak “a” in figure 3.5) was normalized to 452 and compared to the total integration of trans double bond protons ( $\text{H}-\text{C}=\text{C}-\text{H}$ , peak “b” in figure 3.5) of the cinnamoyl group. The degree of polymerization for both Di-block were matching very well to feed M/I. The degree of polymerization and molecular weight of the Di-blocks obtained using NMR are given in Table 3.1.

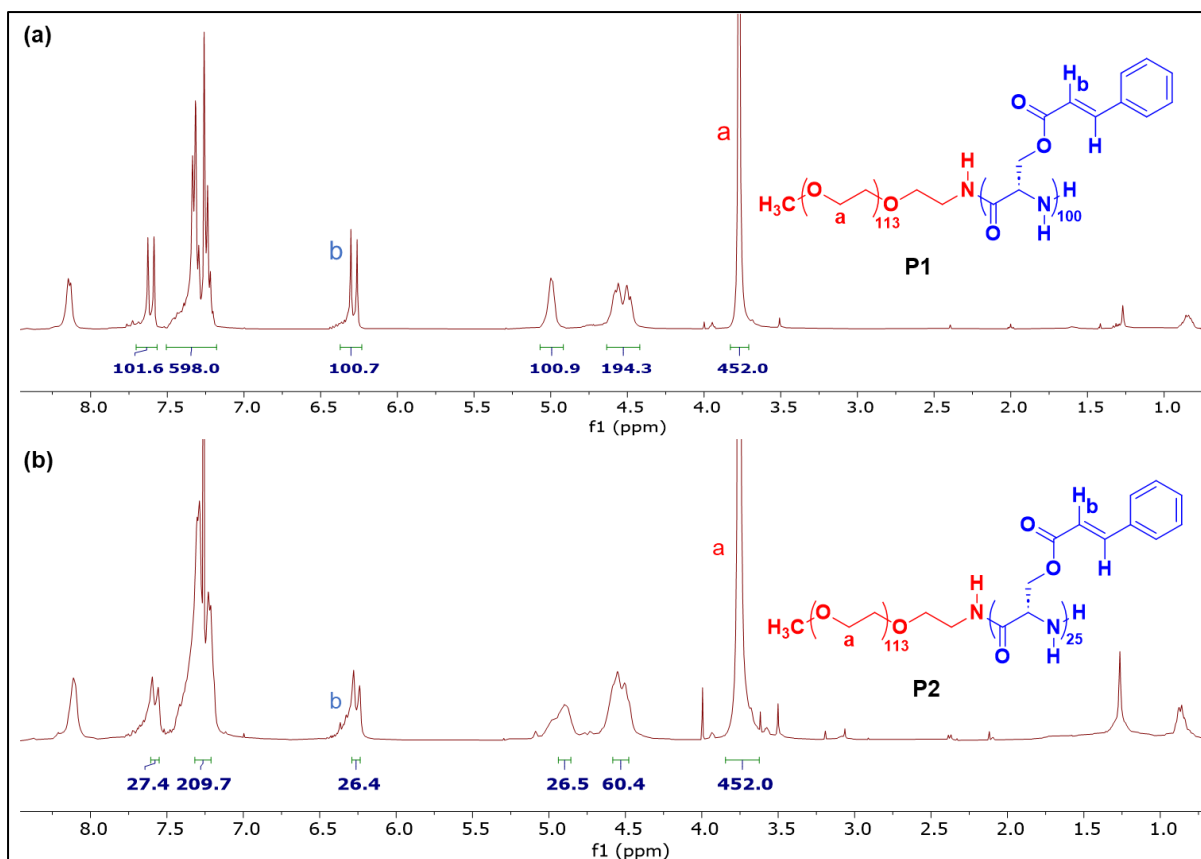


**Figure: 3.5** -  $^1\text{H}$  NMR of Di – block copolymer in  $\text{CDCl}_3$ : (a) PEG-b-P(CSer) $_{100}$ . (b) PEG-b-P(CSer) $_{25}$ .

We were not able to record GPC for polymer **P1** due to solubility issues but it was done for polymer **P2** (Figure 3.6.a). The peak was monomodal and narrow disperse. The degree of polymerization, molecular weight and Dispersity ( $\bar{D}$ ) of the Di-blocks obtained by GPC are given in Table 3.1.

**Table: 3.1** -  $^1\text{H}$  NMR and GPC characterization table

No.	Polymer <sup>a</sup>	M/I (feed)	$X_n$ (NMR)	( $M_n$ (NMR)) <sup>b</sup>	$M_n$ (GPC)	$M_w$ (GPC)	$\bar{D}^c$
1	PEG-b-P(Cser)	25	26	10600	9700	11400	1.2
2	PEG-b-P(Cser)	100	100	26700	<sup>d</sup> -	-	-
3	PEG-b-P(Cser)-b-P(BnGlu)	25:100	25:110	34,500	30700	57400	1.9
4	PEG-b-P(Cser)-b-P(CbzLys)	25:100	25:115	40,600	34100	61600	1.8

<sup>a</sup> Polymerization was carried out in dry  $\text{CHCl}_3$  using PEG-5K amine as an initiator and NHC as the catalyst. <sup>b</sup> $M_n$  (NMR) = 5000 + ( $n^*$  repeating unit mass). <sup>c</sup>GPC data obtained in  $\text{CHCl}_3$  at 25°C with respect to polystyrene standards. <sup>d</sup>Not determined due to insolubility in organic solvents.

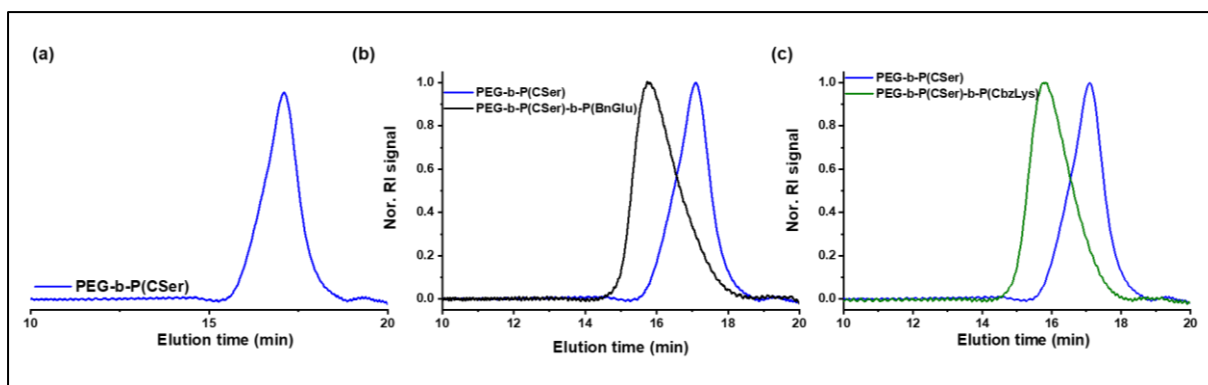


**Figure: 3.6** – GPC plots in  $\text{CDCl}_3$  (a) Di – block copolymer:  $\text{PEG-b-P(CSer)}_{25}$ . (b) Triblock copolymer:  $\text{PEG-b-P(CSer)-b-P(Bn-Glu)}(\mathbf{P3})$ . (c)  $\text{PEG-b-P(CSer)-b-P(CbzLys)}(\mathbf{P4})$ .

To confirm the livingness of polymerization we performed chain extension using other NCA monomers to make tri-block copolymers. The homopolymer **P2** was chosen as a macro-initiator to initiate the polymerization of  $\gamma$ -benzyl glutamate and CBz lysine NCA monomer to produce a tri-block copolymers. In a typical polymerization condition, using PEG-5K amine as initiator, NHC as catalyst at  $25^\circ\text{C}$  under  $\text{N}_2$  atmosphere the serine monomer (**M1**) was polymerized. After completion of polymerization, the second monomer i.e.,  $\gamma$ -benzyl l-glutamate NCA ( $M/I=100$ ) was charged into the polymerization reactor to give the tri-block copolymer  $\text{PEG-b-P(CSer)}_{25}\text{-b-P(BnGlu)}_{100}$  (**P3**) (Scheme 3.3.b). In a similar manner, the addition of CBz-Lys NCA ( $M/I = 100$ ) to the fully grown macro-initiator produced the other tri-block copolymer  $\text{PEG-b-P(CSer)}_{25}\text{-b-P(CbzLys)}_{100}$  (**P4**) (Scheme: 3.3.c). The completion of polymerization was confirmed by FTIR (Figure: 3.4.b for **P4** and 3.4c for **P3**).  $^1\text{H}$  NMR analysis reveals the existence of the expected chemical structure having a degree of polymerization as 25 & 110 in polymer **P3** (Figure: 3.7.a) and 25 & 115 in polymer **P4** (Figure 3.7.b) for second and third block respectively. The degree of polymerization for all the block segments were matching to feed  $M/I$  in both the tri-block copolymers confirms the control in polymerization process.

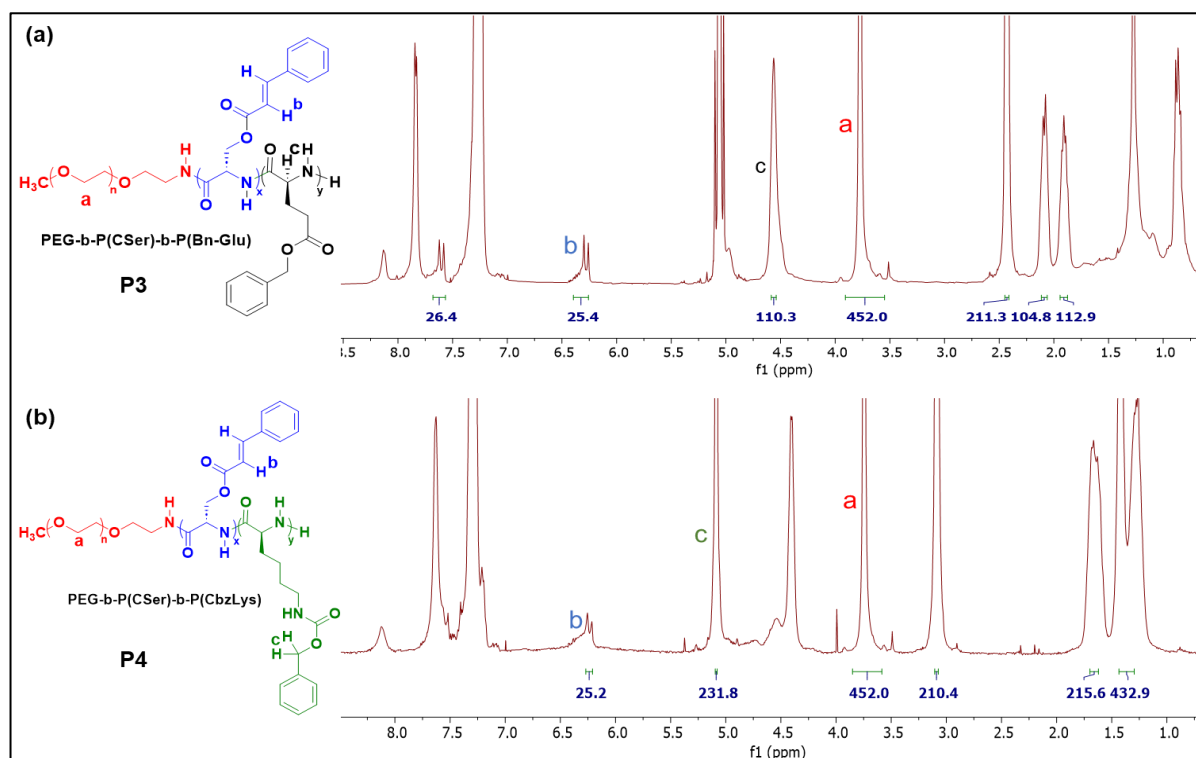


**Figure: 3.7** -  $^1\text{H}$  NMR of tri – block copolymer in  $\text{CDCl}_3$ : (a) PEG-b-P(CSer)-b-P(Bn-Glu)(P3). (b) PEG-b-P(CSer)-b-P(CbzLys)(P4).

Their monomodal GPC chromatograms (Figure 3.6.b and 3.6.c for polymer **P3** and **P4** respectively) with an early elution of tri-block copolymer compared to macroinitiator di-block copolymer strongly suggest better control of the degree of polymerization. The dispersity of the tri-block is good for peptide-based tri-block copolymers. The degree of polymerization (calculated by NMR), molecular weight and Dispersity ( $\bar{D}$ ) of the block copolymer obtained using Gel permeation chromatography is given the Table 3.1. The  $M_n$  of the polymers determined by GPC were found to be less than that expected with  $^1\text{H}$  NMR.

### 3.3. Emulsion Polymerization in Water: ROPISA route

After establishing the polymerizable ability of cinnamoyl serine NCA monomer in organic solvent we further move ahead to polymerize it under ring opening polymerization induced self-assembly (ROPISA) conditions. The serine monomer (**M1**) was subjected to polymerization in aqueous  $\text{NaHCO}_3$  (pH  $\sim$  8.5) solvent using

PEG 5K-amine (MeO-PEG<sub>5000</sub>-NH<sub>2</sub>) as a hydrophilic macroinitiator at various M/I ratios (M/I = 10, 25, 50 and 100) (Figure: 3.8.a). The reaction was carried out at a slightly basic pH in order to favour NCA aminolysis (ring opening of NCA by amine) over NCA hydrolysis (ring opening of NCA by water). Additionally, the amount of monomer and initiator used in the polymerization reaction was chosen in such a way that it produces an emulsion with a total solid content of 7 weight percent at the end of the reaction (i.e., 700 mg of polymer would be made in 10 mL of reaction, assuming total monomer consumption), while also maintaining the desired monomer to initiator ratio (M/I).

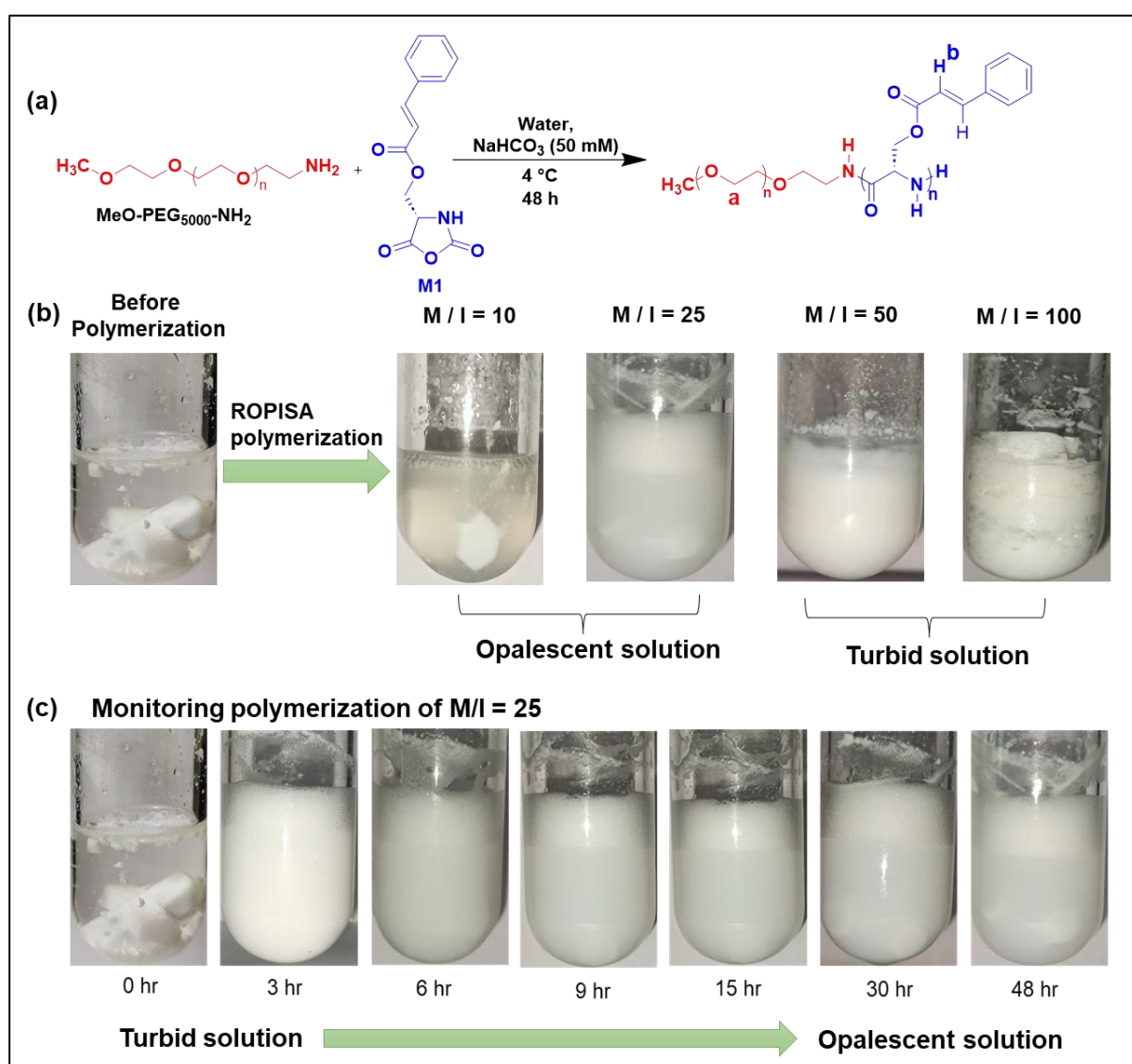


**Figure:3.8** - (a) Synthetic scheme for ROPISA mediated polymerization of Serine NCA monomer **M1** (b) pictures of the polymerization reaction mixture at the start and the

end of polymerization for different M/I ratios. (c) progress of the ROPISA-mediated polymerization reaction for M/I = 25.

In a typical experiment, Serine NCA monomer (**M1**) was introduced to a solution of MeO-PEG<sub>5000</sub>-NH<sub>2</sub> in 50 mM aq. NaHCO<sub>3</sub> at 4°C and rapidly stirred for 48 hours. Due to the monomer's insolubility in water at the beginning, the reaction mixture was a turbid solution however, after 48 hours of stirring, the reaction mixtures were opalescent solutions for polymerization at M/I = 10 (**P10**) and M/I = 25 (**P25**). On the other hand, the reaction medium was turbid for polymerization at M/I = 50 and M/I = 100, indicating a lack of colloidal stability at larger feed ratios and hence they were not studied further. The photographs at the beginning and end of the polymerization reaction are given for all M/I ratios in Figure 3.8.b. The progress of the polymerization reaction from a turbid solution to a blue-tinted opalescent solution for **P25** is shown in Figure: 3.8.c.

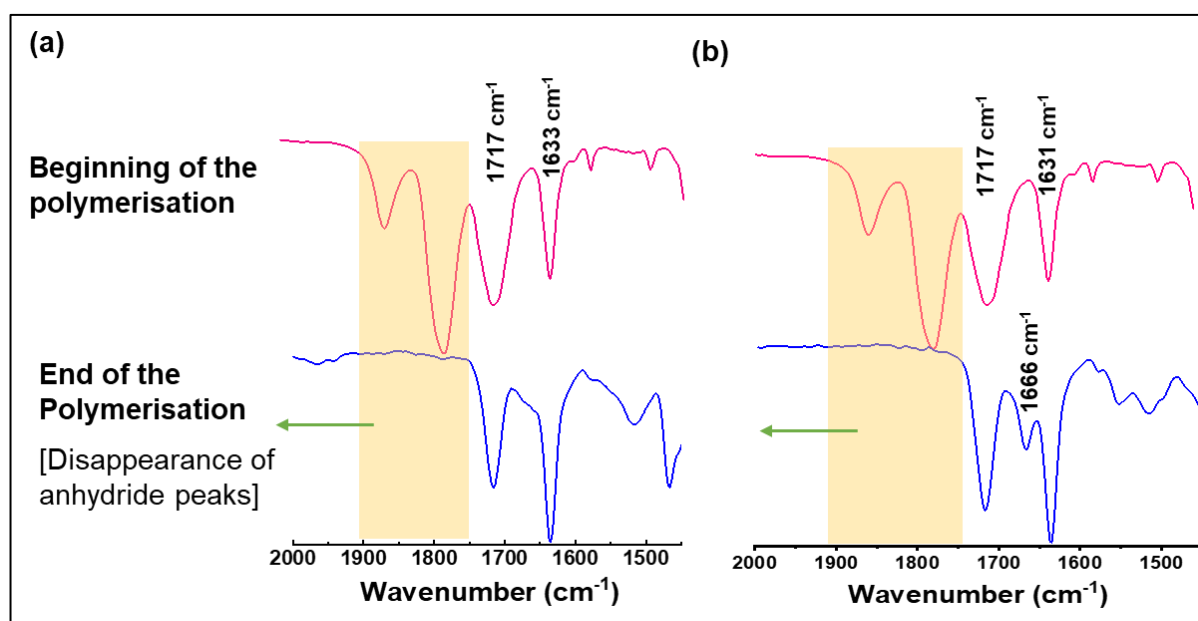


**Figure: 3.9** - FTIR spectra of Di – block copolymer via ROPISA: (a) **P10**. (b) **P25**.

ATIR-FTIR was used to analyse the progress of the reaction. The disappearance of NCA anhydride peaks and the appearance of new peak at amide region (1666 cm<sup>-1</sup>) at the end of 48 hour indicate that the monomer has completely been consumed and that the polymer has formed (Figure: 3.9.a and 3.9.b for **P10** and **P25** respectively, *note that the amide peak emerges with the double bond stretching*

frequency peak in case of **P10**). The resultant di-block copolymers (**P10** and **P25**) underwent dialysis (to remove the  $\text{NaHCO}_3$  salt) followed by lyophilization. The fluffy powder obtained was subjected to  $^1\text{H}$  NMR analysis. The degree of polymerization ( $X_n$ ) was determined by comparing the initiator proton ( $-\text{O}-\text{C}_2\text{H}_4-$ , peak “a” in figure 3.10) normalized to 452, with the total integration of trans double bond protons ( $\text{H}-\text{C}=\text{C}-\text{H}$ , peak “b” in figure 3.10) of the cinnamoyl group. It was found that the degree of polymerization was 12 and 25 for P-10 and P-25 respectively (Figure: 3.10.a and 3.10.b for **P25** and **P10** respectively), indicating the control in polymerization process as it is perfectly matching to feed M/I ratio.

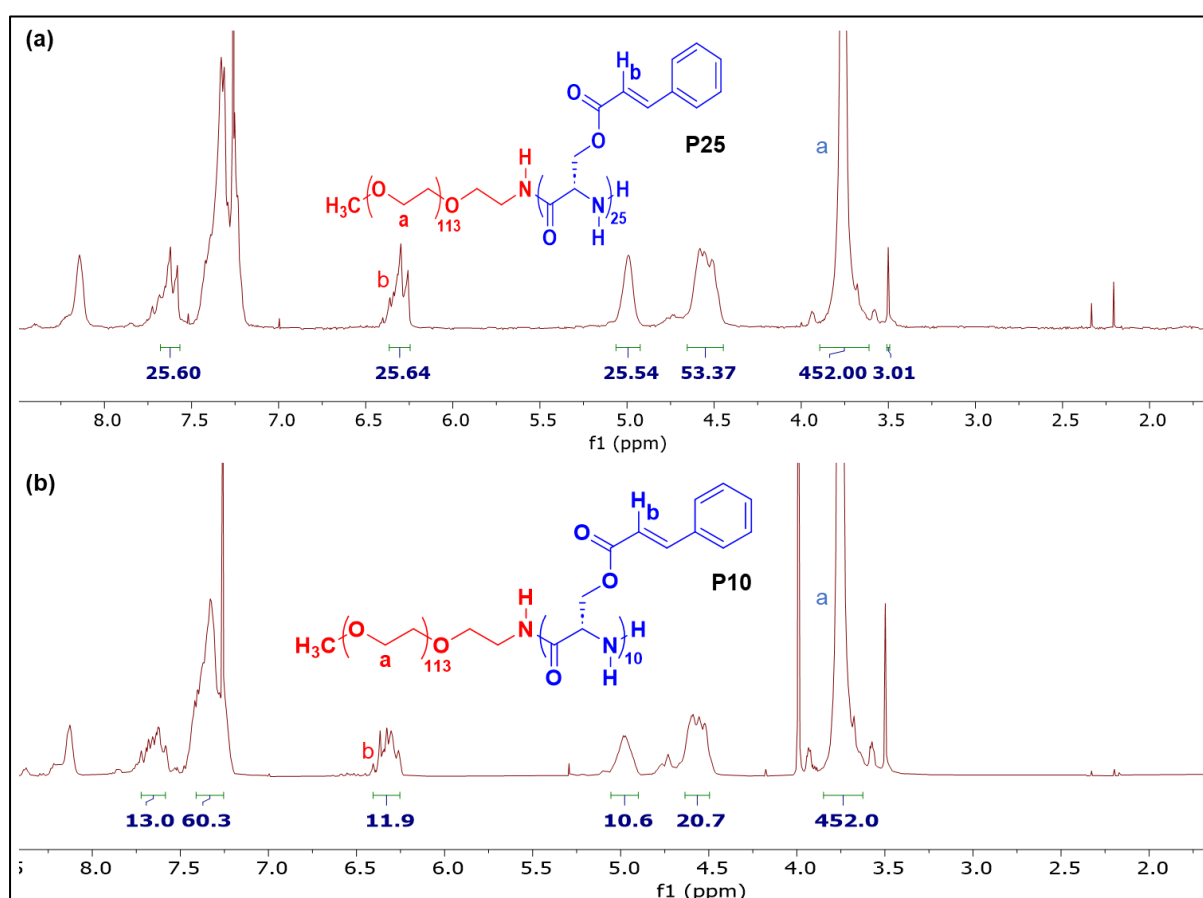


**Figure: 3.10** -  $^1\text{H}$  NMR of Di – block copolymer via ROPISA in  $\text{CHCl}_3$ : (a) PEG-b-P(CSer)<sub>25</sub>. (b) PEG-b-P(CSer)<sub>10</sub>.

Then, **P-10** and **P-25** were subjected to GPC analysis with  $\text{CHCl}_3$  as an eluent. They exhibited monomodal, narrow-dispersed peaks (Figure: 3.11). The dispersity of both the di-blocks were close to theoretical value and the early elution of **P25** over **P10** suggest the control of degree of polymerization of the polymers via ROPISA route.

The degree of polymerization (calculated by NMR), molecular weight and Dispersity ( $\bar{D}$ ) of the block copolymer obtained using GPC is given the Table 3.2. The  $M_n$  of the polymers determined by GPC were found to be in close agreement with that obtained from  $^1\text{H}$  NMR.

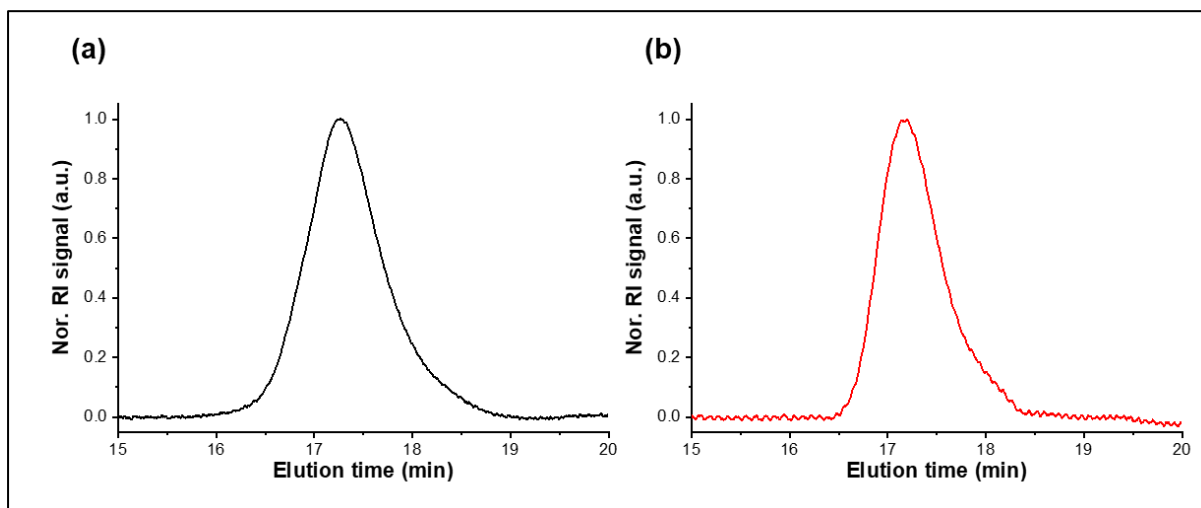


**Figure: 3.11** - GPC plot of Di – block copolymers via ROPISA in  $\text{CHCl}_3$  (a) **P10**. (b) **P25**

**Table: 3.2** -  $^1\text{H}$  NMR and GPC characterization table

No.	Polymer <sup>a</sup>	M/I (feed)	X <sub>n</sub> ( $^1\text{H}$ NMR)	(M <sub>n</sub> (NMR)) <sup>b</sup>	M <sub>n</sub> (GPC)	M <sub>w</sub> (GPC)	$\bar{D}$ <sup>c</sup>
1	P10	10	12	7600	9144	10,890	1.2
2	P25	25	26	10600	9700	11400	1.2
3	P50	50	d <sub>-</sub>	-	-	-	-
4	P100	100	-	-	-	-	-

<sup>a</sup> Polymerization was carried out in 50 mM aq.  $\text{NaHCO}_3$  using PEG-5K amine as an initiator maintaining a total solid content of 7 %. <sup>b</sup>  $M_n$  (NMR) = 5000 + (n\* repeating unit mass). <sup>c</sup> GPC data obtained in  $\text{CHCl}_3$  at 25°C with respect to polystyrene standards. <sup>d</sup> Not determined due to difficulty in isolation.

### 3.4. DLS and morphology

To determine the size and morphology of the nanoparticles formed, it was subjected to DLS, AFM and HR TEM studies. DLS histogram before and after dialysis reveals the existence of nanoscale particles of size around 31 nm (Figure: 3.12.b). The fact that the size was the same before and after dialysis illustrates the stability of the emulsion that was generated via ROPISA procedure. The morphology and size of the generated nanoparticles were then analysed using both AFM and HR TEM



microscopy on the dialysed samples. The HR TEM image shows spherical nano assemblies of the size 25 nm which were coinciding with the DLS size histograms (Figure: 3.12.c), but the AFM images show spherical nanoparticles of about 60 nm (Figure: 3.12.d).

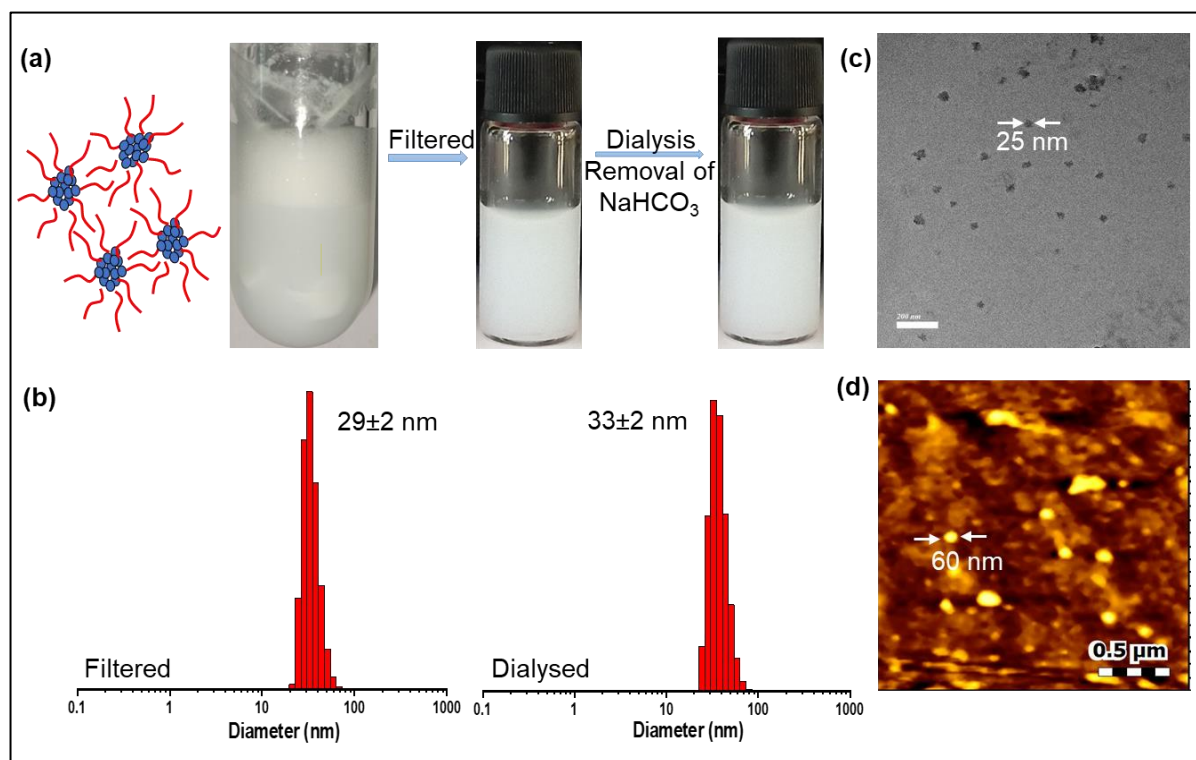


**Figure: 3.12** – Size and morphology study of **P25** – (a) Scheme depicting stability of nano assemblies generated by ROPISA. (b) DLS histograms for filtered and dialysed ROPISA sample. (c) HR-TEM (d) AFM images of dialysed samples.

### 3.5. Micelle formation and CMC study

It is well known that in a specific solvent, block polypeptides that are amphiphilic can self-assemble into micelles and vesicles. But in the case of ROPISA technique micelles are formed during the progress of the polymerization reaction itself. Here, the block copolymers are made of a hydrophobic P(CSer) block that will be confined in the micelle core while the very hydrophilic PEG block will make up the micelle's outer corona. Using the well-known pyrene probe-based fluorescence approach, the excitation spectra of pyrene with increasing concentrations of block copolymer (**P25**)

was examined to show the development of micelles. The fluorescence intensity ratio of  $I_{371}/I_{381}$  versus concentration of the copolymer was plotted, and the point of intersection of the tangent lines drawn to the horizontal line with a constant intensity ratio and to the diagonal line where the intensity ratio is rapidly increasing was used to determine the CMC value (Figure 3.13.a). The CMC value obtained was 1.2  $\mu\text{g/mL}$ .  $^1\text{H}$  NMR was also used to confirm the self-assembly of the block copolymer **P25**. To achieve this,  $\text{D}_2\text{O}$  was used as the solvent during the polymerization, while maintaining all other conditions. In contrast to the  $^1\text{H}$  NMR recorded in  $\text{CHCl}_3$  (Figure: 3.10.a), all of the P(CSer) peaks disappear in  $\text{D}_2\text{O}$  (Figure: 3.13.b), while all of the PEG peaks are still present. It implies that the P(CSer) segments constitute the micelle's core and cannot be detected by  $^1\text{H}$  NMR in  $\text{D}_2\text{O}$ , whereas the PEG segments make up the micelle's outer corona and remain in a solvated state, making them detectable in  $^1\text{H}$  NMR spectra.

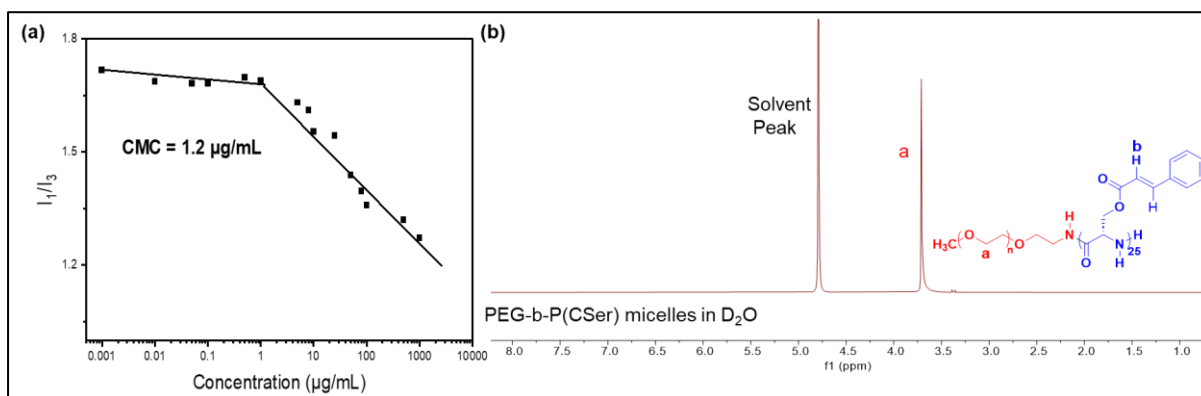


**Figure: 3.13** – (a) intensity ratio ( $I_{371}/I_{382}$ ) as a function of concentration PEG-b-P(CSer)<sub>25</sub> synthesised via ROPISA. (b)  $^1\text{H}$  NMR of PEG-b-P(CSer) synthesised via ROPISA in  $\text{D}_2\text{O}$ .

### 3.6. Photo crosslinking strategy, verification and its effect on the size

There have been substantial studies on the photochemistry of coumarin and cinnamoyl groups. Both functional groups can be photo-dimerized by  $[2 + 2]$  cycloaddition under UV illumination of  $\lambda > 260$  nm, producing a cyclobutane ring. The photodimerization of the cinnamoyl moiety on polypeptides has, however, received little attention. In this work, polypeptides are made from monomers (NCA) that have already undergone cinnamoyl moiety modification.

To investigate photodimerization, the micelle solution of PEG-b-P(CSer)<sub>25</sub> at a concentration of 1 mg/mL (in MilliQ) in a Petri dish was subjected to UV irradiation at 265 nm (Figure: 3.14.a). To understand degree of polymer crosslinking, the absorbance of PEG-b-P(CSer)<sub>25</sub> was tracked as a function of UV exposure time. The absorption peak at 285 nm declined steadily with UV-irradiation time (Figure 3.15.a), indicating the [2 + 2] photocycloaddition reactions of the cinnamoyl group which destroys conjugation in the entire pi-electron system (Figure: 3.14.b). It is noteworthy to notice that all particles were distributed effectively indicating that the cross-linking reaction between the micelles did not cause micellar aggregation.

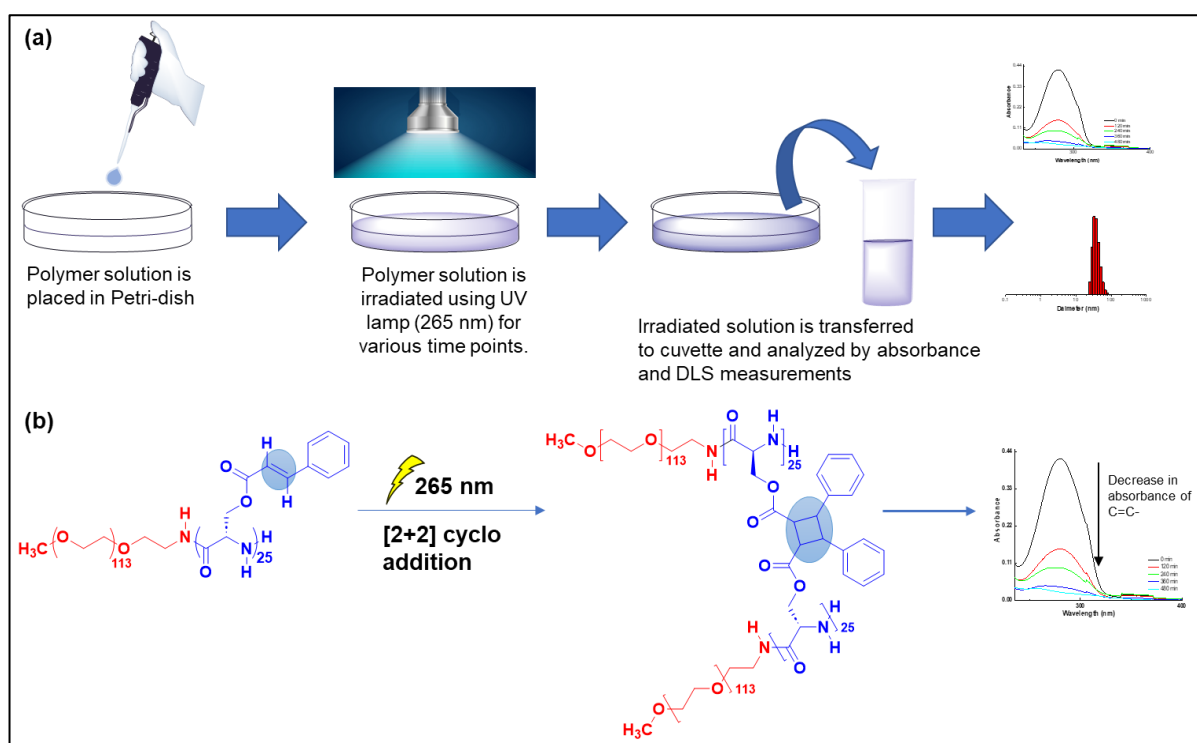


**Figure: 3.14** – (a) pictorial representation of strategy and verification methods of photo crosslinking. (b) Schematic representation of photo crosslinking of the block copolymer (P25) through [2+2] cyclo addition.

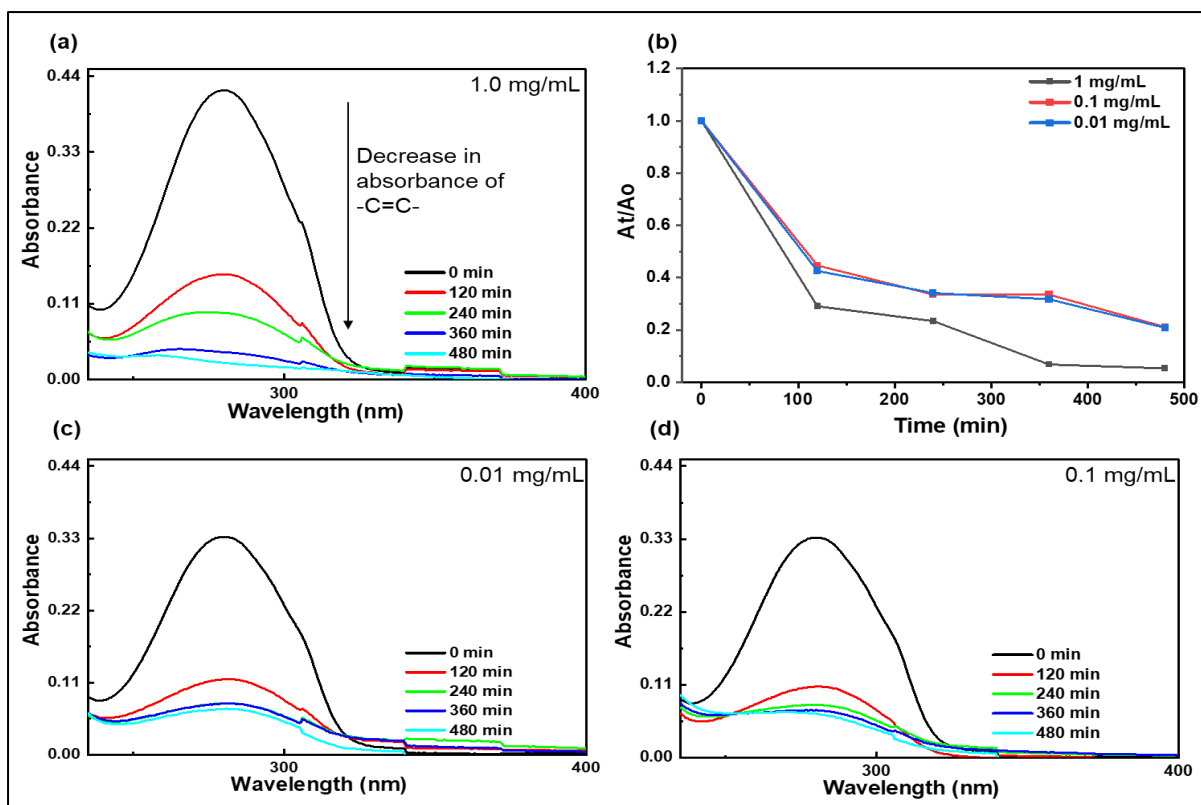


**Figure: 3.15** – (a) UV-Vis spectra of ROPISA sample PEG-b-P(CSer)<sub>25</sub> against irradiation time for 1 mg/mL. (b) Plot of  $A(t)/A(0)$  at 285 nm v/s irradiation time. (c) UV-Vis spectra of ROPISA sample PEG-b-P(CSer)<sub>25</sub> against irradiation time for 0.01 mg/mL. (d) 0.1 mg/mL.

Additionally,  $A(t)/A(0)$  against irradiation time was also plotted, where  $A(t)$  and  $A(0)$  represents absorbance at 285 nm during time  $t$  and 0 respectively (Figure: 3.15.b). It is evident from the plot that, most of the curing happened within the first two hours and there was only a small increment in the crosslinking degree beyond that period.

The same approach was administrated for polymer sample of different concentrations. It was found that the outcomes were consistent regardless of the concentration used, and that the degree of crosslinking was greater when the concentration was 1 mg/ml. Therefore, we continued our further crosslinking studies at 1 mg/mL polymer concentration. (Figure: 3.14.c and 3.14.d for 0.01 mg/mL and 0.1 mg/mL respectively).

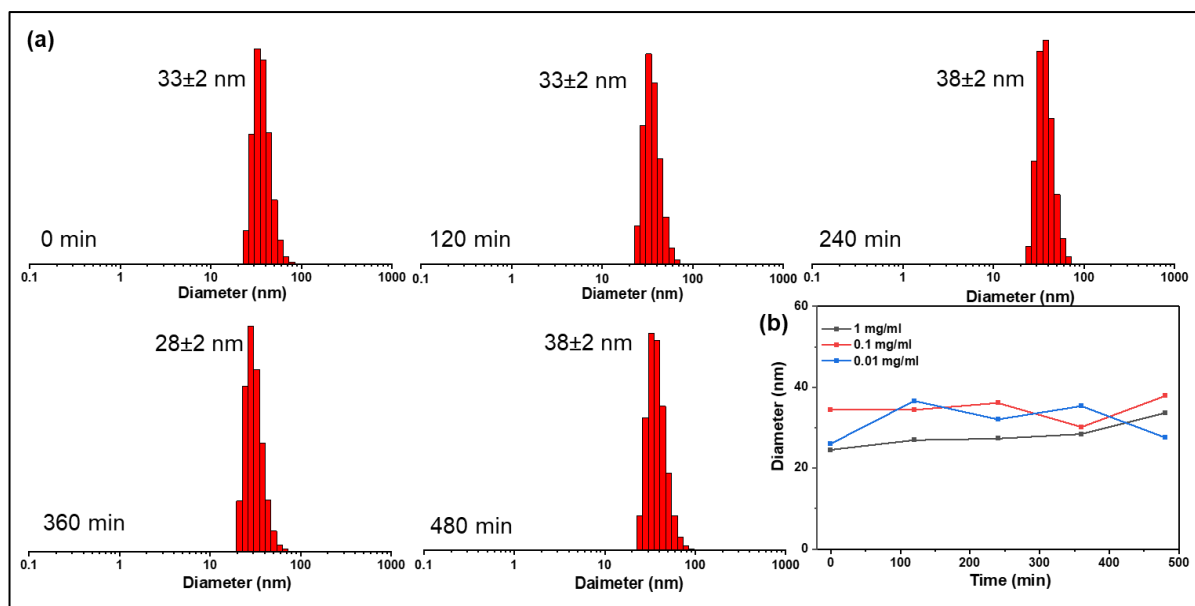


**Figure: 3.16** – (a) DLS histograms of ROPISA sample PEG-b-P(CSer)<sub>25</sub> for different time interval at a concentration of 1 mg/mL. (b) Plot of diameter against irradiation time for different concentration of **P25** polymer.

DLS measurements were used to determine the diameter of the PEG-b-P(CSer) nano assembly that was subjected to photo crosslinking (Figure 3.16.a). All had a hydrodynamic diameter of approximately 33 nm. These findings shows that PEG-b-P(CSer) self-assembled into micelles, and further photo crosslinking had little effect on the physical properties of the nano assemblies. Additionally, it was confirmed using samples with various concentrations (Figure: 3.16.b plot shows the diameter against irradiation time for varying concentration of **P25**). Independent of concentration, the diameter variation during the crosslinking process is negligible. At the end of the eighth hour, TEM and AFM images of the crosslinked nanoparticle were taken. TEM showed spherical nano assemblies with a diameter of 30 nm, whereas nanoparticle with spherical morphology of 65 nm size was obtained from AFM images (Figure 3.17.a and 3.17.b respectively). They were perfectly coinciding with the TEM and AFM data obtained before crosslinking. Thus, confirming that the physical properties of the micelles formed by **P25** via ROPISA route doesn't change due to photo crosslinking.

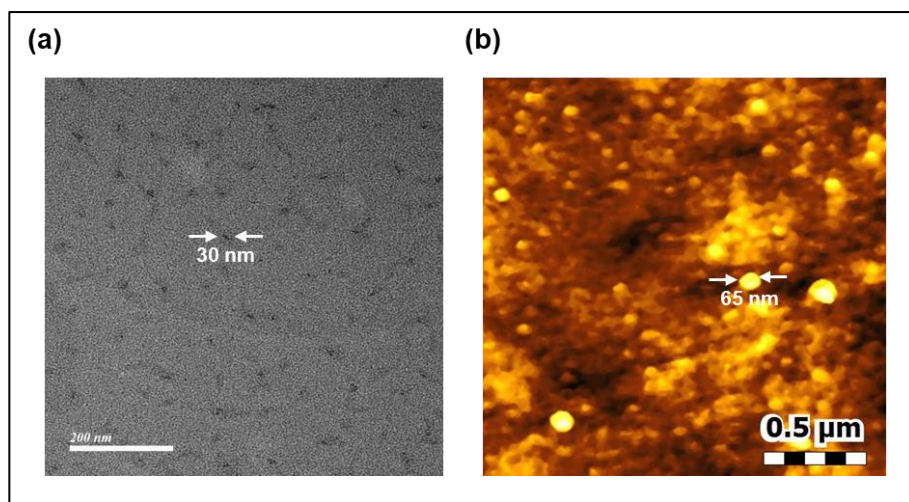


**Figure: 3.17** – Morphology and size of crosslinked ROPISA sample **P25** (a) HR TEM (b) AFM images of crosslinked nanoparticles.

### 3.7. ROPISA driven encapsulation strategy

In order to move the ROPISA and photo crosslinking strategy to an application level the encapsulation of dye during the ROPISA process was investigated, and the impact of crosslinking on these loaded samples will be addressed. For this the first task was to make dye loaded nanoparticles. We hypothesised that, if dye molecule is introduced at the beginning of ROPISA mediated polymerization along with monomer, they will also get trapped inside the initially formed nano assemblies of amphiphilic oligomers. Additionally, polymerization will continue until the monomer is consumed and at the end, an emulsion made of dye molecules enclosed in nanoscale polymer assemblies will be generated (Figure: 3.18). I used a total of two dyes for these studies and among them, Nile Red is water insoluble and Rhodamine B is water soluble dye.

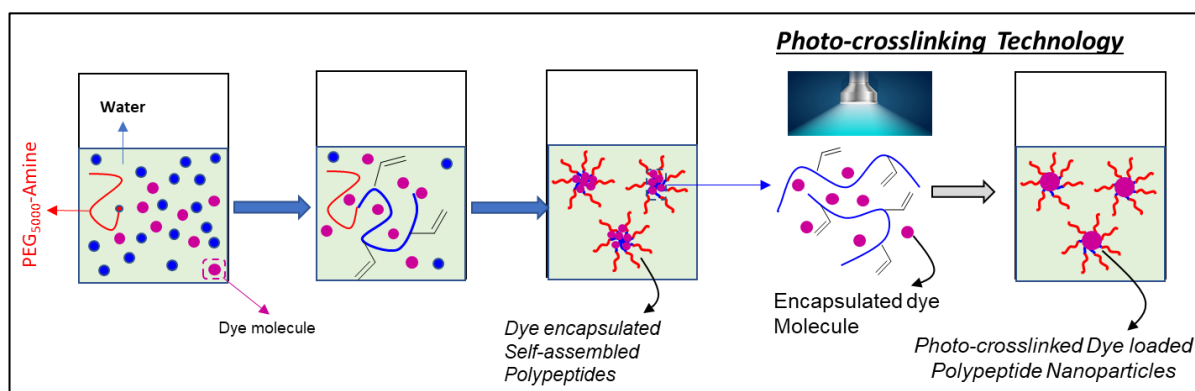




**Figure: 3.18** – Pictorial representation depicting the ROPISA driven encapsulation method and photo crosslinking impact on this dye loaded nanoparticles.

Under the same conditions as previously described, the monomer **M1** was polymerized using PEG 5k amine as the macroinitiator at M/I = 25, and the dye molecule was introduced at the start of ROPISA-driven polymerization. This is remarkable because, during the polymerization process, dye molecules can be enclosed in polymer nano-assemblies. The reaction mixture was filtered after polymerization to remove unencapsulated water-insoluble dye molecules, and then half of it was extensively dialysed for 48 h. The dialysed suspension was filtered once again and used for analysis (Figures 3.19.a and 3.20.a shows the progression of the reaction till dialysis for Rhodamine B and Nile Red respectively).

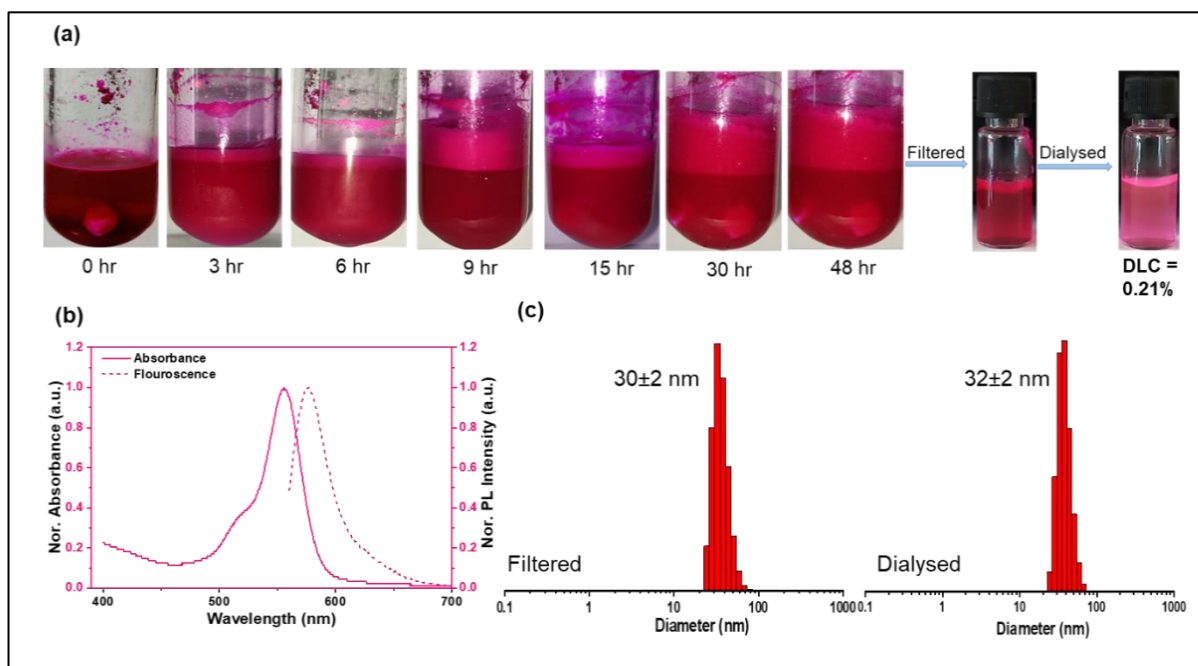


**Figure 3.19** – data for Rhodamine B loaded polymer emulsion (a) progress of the reaction including filtration and dialysis. (b) Absorption and Emission spectra. (c) DLS histogram of filtered and dialysed dye loaded nano assemblies.

Absorbance and fluorescence were measured for dye-loaded emulsion and their spectra were plotted. Rhodamine B and Nile Red loaded polymer emulsions had absorption peaks at 550 nm, but their fluorescence peaks were at 577 nm and 614 nm, respectively, implying that Nile Red-loaded emulsion had a larger stoke shift

(Figures 3.19.b and 3.20.b shows absorbance as well as emission spectra of Rhodamine B and Nile Red respectively).

The dye-loaded emulsions were subjected to DLS measurements before and after dialysis and the sizes of resultant dye-loaded nano assemblies were measured (Figure 3.19.c and 3.20.c for Rhodamine B and Nile Red loaded assemblies respectively). The diameters of dye-loaded nano assemblies were exactly identical to those of nascent nano assemblies of polymers. The size of the dialysed and undialysed dye-loaded samples was also the same, suggesting the stability of the encapsulated samples.

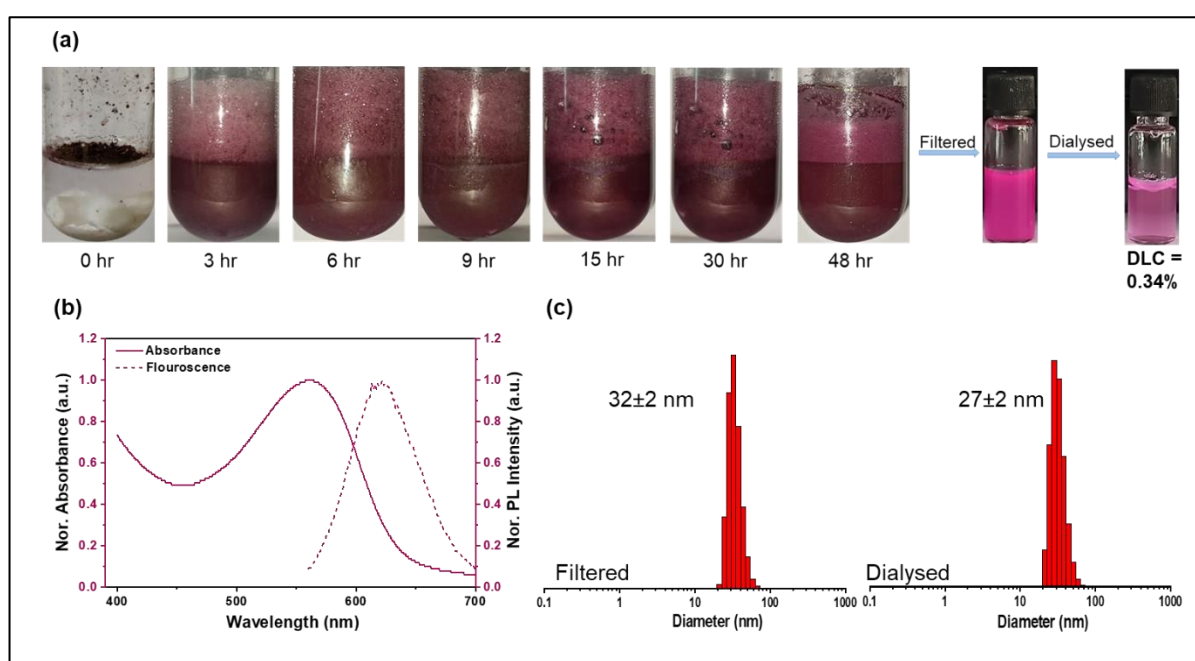


**Figure 3.20** – data for Nile Red loaded polymer emulsion (a) progress of the reaction including filtration and dialysis. (b) Absorption and Emission spectra. (c) DLS histogram of filtered and dialysed dye loaded nano assemblies.

Furthermore, in order to quantify the amount of dye in the nano assemblies the Dye loading capacity (DLC) was computed using the absorbance data of the dye-loaded samples. The DLC values were lower than expected. Now, the photo crosslinked dye-encapsulated nanoparticle's dye loading capability needs to be evaluated. We anticipate that the loading capacity will alter significantly after crosslinking. ROPISA route would be tested for in-situ cross-linking and loading of dye molecules and their preliminary biomedical applications will be attempted.



## 4. Conclusion

The cinnamoyl functionalised amino acid was converted into its  $\alpha$ -amino acid-N-carboxyanhydride using the moisture tolerant route developed by Hua lu and co-workers. The NCA was transformed into its corresponding PEG di-block polypeptide using PEG<sub>5K</sub>-amine as an initiator, and then into a tri-block copolymer employing benzyl glutamate and CBz lysine NCA. <sup>1</sup>H NMR and GPC were used to characterize the polymers. The degree of polymerization was in close agreement with feed M/I ratio, and block copolymers exhibited monomodal and narrow disperse GPC profile. The serine-based NCA monomer was then polymerized using the aqueous ROPISA method in 50 mM aq. NaHCO<sub>3</sub> solution and PEG-amine as an initiator. For M/I = 10 and 25, stable opalescent emulsions could be generated after experimenting with various M/I ratios. The degree of polymerization of isolated di-block copolymers from these stable emulsions closely matched with feed M/I ratio, and exhibited monomodal and narrow disperse GPC profile. According to DLS measurements, the **P10** and **P25** di-blocks were both made up of nano-assemblies that were between 25 and 30 nm in size and these nano-assemblies were found to exist in spherical nanoparticle morphology based on our HR-TEM and AFM analysis. Photo crosslinking of these nano assemblies were done using UV light of wavelength 265 nm and it was verified using UV-Vis spectroscopy. When light falls on these ROPISA mediated di-block samples, the cinnamoyl group in the sidechain of the polymer undergoes [2+2] cycloaddition to form cyclobutene rings which results in the formation of crosslinked nanoparticles. The crosslinking is confirmed by the steady decline of the absorption peak at 285 nm that corresponds to the -C=C- bond. DLS measurement shows that the size of the crosslinked nanoparticles is unchanged even after 8 h of curing, indicating that the physical properties remain intact even after photo crosslinking. This was further supported by HR TEM and AFM images, which displayed spherical nanoparticles that were comparable in size to uncross-linked nano assemblies. This approach was used to create Nile Red and Rhodamine B loaded nano particles by adding dye at the beginning of the polymerization process. These results are promising, and the eco-friendly method of creating polymers based on polypeptides would increase the potential for polypeptide-based nanomaterials in biomedical applications.

## 5. References

- (1) Dau, H.; Jones, G. R.; Tsogtgerel, E.; Nguyen, D.; Keyes, A.; Liu, Y.-S.; Rauf, H.; Ordonez, E.; Puchelle, V.; Basbug Alhan, H. Linear Block Copolymer Synthesis. *Chemical Reviews* **2022**, 122 (18), 14471–14553.
- (2) Mai, Y.; Eisenberg, A. Self-Assembly of Block Copolymers. *Chemical Society Reviews* **2012**, 41 (18), 5969–5985. <https://doi.org/10.1039/C2CS35115C>.
- (3) Dionzou, M.; Morère, A.; Roux, C.; Lonetti, B.; Marty, J.-D.; Mingotaud, C.; Joseph, P.; Goudounèche, D.; Payré, B.; Léonetti, M. Comparison of Methods for the Fabrication and the Characterization of Polymer Self-Assemblies: What Are the Important Parameters? *Soft Matter* **2016**, 12 (7), 2166–2176.
- (4) Gil-Ramírez, G.; Benet-Buchholz, J.; Escudero-Adán, E. C.; Ballester, P. Solid-State Self-Assembly of a Calix[4]Pyrrole–Resorcinarene Hybrid into a Hexameric Cage. *J. Am. Chem. Soc.* **2007**, 129 (13), 3820–3821. <https://doi.org/10.1021/ja070037k>.
- (5) Rodriguez-Hernandez, J.; Chécot, F.; Gnanou, Y.; Lecommandoux, S. Toward ‘Smart’ Nano-Objects by Self-Assembly of Block Copolymers in Solution. *Progress in polymer science* **2005**, 30 (7), 691–724.
- (6) Lu, Y.; Lin, J.; Wang, L.; Zhang, L.; Cai, C. Self-Assembly of Copolymer Micelles: Higher-Level Assembly for Constructing Hierarchical Structure. *Chemical reviews* **2020**, 120 (9), 4111–4140.
- (7) Penfold, N. J.; Yeow, J.; Boyer, C.; Armes, S. P. Emerging Trends in Polymerization-Induced Self-Assembly. *ACS Macro Letters* **2019**, 8 (8), 1029–1054.
- (8) Canning, S. L.; Smith, G. N.; Armes, S. P. A Critical Appraisal of RAFT-Mediated Polymerization-Induced Self-Assembly. *Macromolecules* **2016**, 49 (6), 1985–2001.
- (9) Derry, M. J.; Fielding, L. A.; Armes, S. P. Polymerization-Induced Self-Assembly of Block Copolymer Nanoparticles via RAFT Non-Aqueous Dispersion Polymerization. *Progress in Polymer Science* **2016**, 52, 1–18.

- (10) Ferguson, C. J.; Hughes, R. J.; Pham, B. T.; Hawzett, B. S.; Gilbert, R. G.; Serelis, A. K.; Such, C. H. Effective Ab Initio Emulsion Polymerization under RAFT Control. *Macromolecules* **2002**, 35 (25), 9243–9245.
- (11) Wan, W.-M.; Hong, C.-Y.; Pan, C.-Y. One-Pot Synthesis of Nanomaterials via RAFT Polymerization Induced Self-Assembly and Morphology Transition. *Chemical Communications* **2009**, No. 39, 5883–5885.
- (12) Cornel, E. J.; Jiang, J.; Chen, S.; Du, J. Principles and Characteristics of Polymerization-Induced Self-Assembly with Various Polymerization Techniques. *CCS Chemistry* **2021**, 3 (4), 2104–2125.
- (13) Wright, D. B.; Touve, M. A.; Adamiak, L.; Gianneschi, N. C. ROMPISA: Ring-Opening Metathesis Polymerization-Induced Self-Assembly. *ACS Macro Letters* **2017**, 6 (9), 925–929.
- (14) Warren, N. J.; Armes, S. P. Polymerization-Induced Self-Assembly of Block Copolymer Nano-Objects via RAFT Aqueous Dispersion Polymerization. *Journal of the American Chemical Society* **2014**, 136 (29), 10174–10185.
- (15) Derry, M. J.; Fielding, L. A.; Armes, S. P. Industrially-Relevant Polymerization-Induced Self-Assembly Formulations in Non-Polar Solvents: RAFT Dispersion Polymerization of Benzyl Methacrylate. *Polymer Chemistry* **2015**, 6 (16), 3054–3062.
- (16) Jones, E. R.; Semsarilar, M.; Blanazs, A.; Armes, S. P. Efficient Synthesis of Amine-Functional Diblock Copolymer Nanoparticles via RAFT Dispersion Polymerization of Benzyl Methacrylate in Alcoholic Media. *Macromolecules* **2012**, 45 (12), 5091–5098.
- (17) Fielding, L. A.; Lane, J. A.; Derry, M. J.; Mykhaylyk, O. O.; Armes, S. P. Thermo-Responsive Diblock Copolymer Worm Gels in Non-Polar Solvents. *Journal of the American Chemical Society* **2014**, 136 (15), 5790–5798.
- (18) Lovett, J. R.; Warren, N. J.; Armes, S. P.; Smallridge, M. J.; Cracknell, R. B. Order–Order Morphological Transitions for Dual Stimulus Responsive Diblock Copolymer Vesicles. *Macromolecules* **2016**, 49 (3), 1016–1025.

- (19) Xu, S.; Yeow, J.; Boyer, C. Exploiting Wavelength Orthogonality for Successive Photoinduced Polymerization-Induced Self-Assembly and Photo-Crosslinking. *ACS Macro Letters* **2018**, 7 (11), 1376–1382.
- (20) Phan, H.; Taresco, V.; Penelle, J.; Couturaud, B. Polymerisation-Induced Self-Assembly (PISA) as a Straightforward Formulation Strategy for Stimuli-Responsive Drug Delivery Systems and Biomaterials: Recent Advances. *Biomaterials Science* **2021**, 9 (1), 38–50.
- (21) Zhu, C.; Nicolas, J. (Bio) Degradable and Biocompatible Nano-Objects from Polymerization-Induced and Crystallization-Driven Self-Assembly. *Biomacromolecules* **2022**, 23 (8), 3043–3080.
- (22) Mazo, A. R.; Allison-Logan, S.; Karimi, F.; Chan, N. J.-A.; Qiu, W.; Duan, W.; O'Brien-Simpson, N. M.; Qiao, G. G. Ring Opening Polymerization of  $\alpha$ -Amino Acids: Advances in Synthesis, Architecture and Applications of Polypeptides and Their Hybrids. *Chemical society reviews* **2020**, 49 (14), 4737–4834.
- (23) Deng, C.; Wu, J.; Cheng, R.; Meng, F.; Klok, H.-A.; Zhong, Z. Functional Polypeptide and Hybrid Materials: Precision Synthesis via  $\alpha$ -Amino Acid N-Carboxyanhydride Polymerization and Emerging Biomedical Applications. *Progress in Polymer Science* **2014**, 39 (2), 330–364.
- (24) Cheng, J.; Deming, T. J. Synthesis of Polypeptides by Ring-Opening Polymerization of  $\alpha$ -Amino Acid N-Carboxyanhydrides. *Peptide-based materials* **2012**, 1–26.
- (25) Deming, T. J. Facile Synthesis of Block Copolypeptides of Defined Architecture. *Nature* **1997**, 390 (6658), 386–389.
- (26) Sun, Y.; Hou, Y.; Zhou, X.; Yuan, J.; Wang, J.; Lu, H. Controlled Synthesis and Enzyme-Induced Hydrogelation of Poly (l-Phosphotyrosine) s via Ring-Opening Polymerization of  $\alpha$ -Amino Acid N-Carboxyanhydride. *ACS Macro Letters* **2015**, 4 (9), 1000–1003.
- (27) Yuan, J.; Zhang, Y.; Li, Z.; Wang, Y.; Lu, H. A S-Sn Lewis Pair-Mediated Ring-Opening Polymerization of  $\alpha$ -Amino Acid N-Carboxyanhydrides: Fast Kinetics, High

Molecular Weight, and Facile Bioconjugation. *ACS Macro Letters* **2018**, 7 (8), 892–897.

(28) Wu, Y.-M.; Zhang, W.-W.; Zhou, R.-Y.; Chen, Q.; Xie, C.-Y.; Xiang, H.-X.; Sun, B.; Zhu, M.-F.; Liu, R.-H. Facile Synthesis of High Molecular Weight Polypeptides via Fast and Moisture Insensitive Polymerization of  $\alpha$ -Amino Acid n-Carboxyanhydrides. *Chinese Journal of Polymer Science* **2020**, 38, 1131–1140.

(29) Li, K.; Li, Z.; Shen, Y.; Fu, X.; Chen, C.; Li, Z. Organobase 1, 1, 3, 3-Tetramethyl Guanidine Catalyzed Rapid Ring-Opening Polymerization of  $\alpha$ -Amino Acid N-Carboxyanhydrides Adaptive to Amine, Alcohol and Carboxyl Acid Initiators. *Polymer Chemistry* **2022**, 13 (5), 586–591.

(30) Jiang, J.; Zhang, X.; Fan, Z.; Du, J. Ring-Opening Polymerization of N-Carboxyanhydride-Induced Self-Assembly for Fabricating Biodegradable Polymer Vesicles. *ACS Macro Letters* **2019**, 8 (10), 1216–1221.

(31) Duro-Castano, A.; Rodríguez-Arco, L.; Ruiz-Pérez, L.; De Pace, C.; Marchello, G.; Noble-Jesus, C.; Battaglia, G. One-Pot Synthesis of Oxidation-Sensitive Supramolecular Gels and Vesicles. *Biomacromolecules* **2021**, 22 (12), 5052–5064.

(32) Gazon, C.; Salas-Ambrosio, P.; Antoine, S.; Ibarboure, E.; Sandre, O.; Clulow, A. J.; Boyd, B. J.; Grinstaff, M. W.; Lecommandoux, S.; Bonduelle, C. Aqueous ROPISA of  $\alpha$ -Amino Acid N-Carboxyanhydrides: Polypeptide Block Secondary Structure Controls Nanoparticle Shape Anisotropy. *Polymer Chemistry* **2021**, 12 (43), 6242–6251.

(33) Gazon, C.; Salas-Ambrosio, P.; Ibarboure, E.; Buol, A.; Garanger, E.; Grinstaff, M. W.; Lecommandoux, S.; Bonduelle, C. Aqueous Ring-Opening Polymerization-Induced Self-Assembly (ROPISA) of N-Carboxyanhydrides. *Angewandte Chemie* **2020**, 132 (2), 632–636.

(34) Hoyle, C. E.; Bowman, C. N. Thiol–Ene Click Chemistry. *Angewandte Chemie International Edition* **2010**, 49 (9), 1540–1573.  
<https://doi.org/10.1002/anie.200903924>.

- (35) Yan, L.; Yang, L.; He, H.; Hu, X.; Xie, Z.; Huang, Y.; Jing, X. Photo-Cross-Linked MPEG-Poly( $\gamma$ -Cinnamyl-L-Glutamate) Micelles as Stable Drug Carriers. *Polym. Chem.* **2012**, 3 (5), 1300–1307. <https://doi.org/10.1039/C2PY20049J>.
- (36) Liu, Q.; Locklin, J. L. Photocross-Linking Kinetics Study of Benzophenone Containing Zwitterionic Copolymers. *ACS Omega* **2020**, 5 (16), 9204–9211. <https://doi.org/10.1021/acsomega.9b04493>.
- (37) Yagci, B. B.; Zorlu, Y.; Türkmen, Y. E. Template-Directed Photochemical Homodimerization and Heterodimerization Reactions of Cinnamic Acids. *J. Org. Chem.* **2021**, 86 (18), 13118–13128. <https://doi.org/10.1021/acs.joc.1c01534>.
- (38) Balaji, R.; Grande, D.; Nanjundan, S. Photocrosslinkable Copolymers Based on 4-Acryloyloxyphenyl-3'-Chlorostyryl Ketone and Methyl Methacrylate: Synthesis, Comonomer Reactivity Ratios and UV Photosensitivity. *Polymer International* **2004**, 53 (11), 1735–1743. <https://doi.org/10.1002/pi.1550>.
- (39) Balaji, R.; Grande, D.; Nanjundan, S. Photoresponsive Polymers Having Pendant Chlorocinnamoyl Moieties: Synthesis, Reactivity Ratios and Photochemical Properties. *Polymer* **2004**, 45 (4), 1089–1099.
- (40) Ding, J.; Zhuang, X.; Xiao, C.; Cheng, Y.; Zhao, L.; He, C.; Tang, Z.; Chen, X. Preparation of Photo-Cross-Linked PH-Responsive Polypeptide Nanogels as Potential Carriers for Controlled Drug Delivery. *J. Mater. Chem.* **2011**, 21 (30), 11383–11391. <https://doi.org/10.1039/C1JM10391A>.